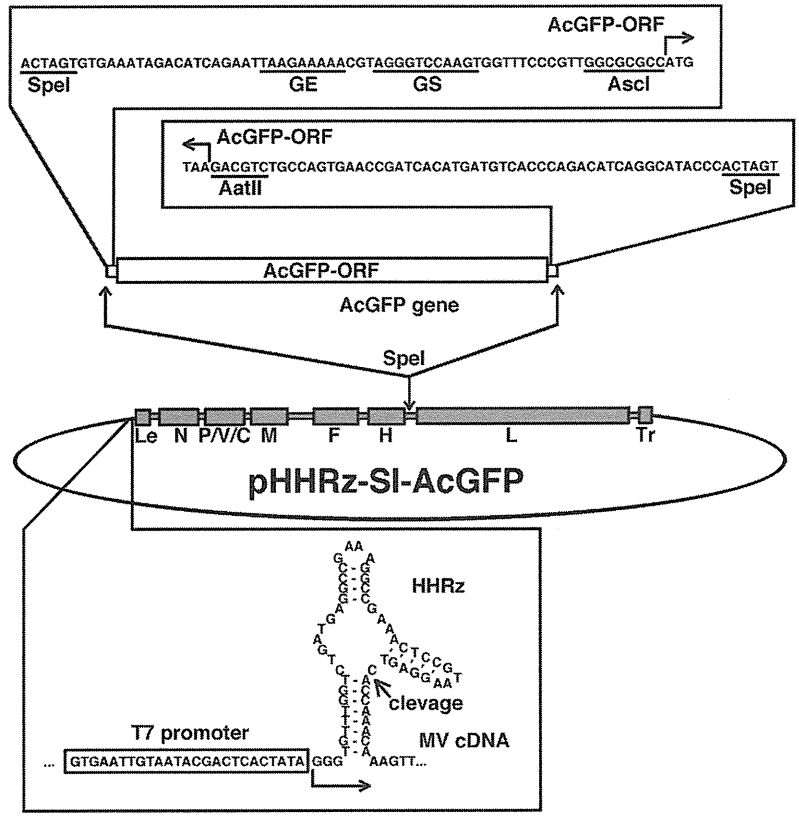

FIG. 2. Diagram of the genome plasmid with insertion of an additional transcriptional unit and the HHRz sequence. Transcriptional regulatory regions (gene end [GE], intergenic, and gene start [GS] sequences) and the coding sequence for AcGFP (AcGFP-ORF) were inserted at the junction between the H and L genes by the use of appropriate restriction enzyme recognition sites (SpeI, AscI, and AatII). The recombinant genome also possesses an HHRz upstream the authentic virus genome.

enome, a precise 5′ end for the MV antigenome was created by inserting HHRz between the three guanines and the first viral nucleotide (Fig. 2). The resulting full-length genome plasmid was designated pHHRz-SI-AcGFP. BHK/T7-9 cells, which represent a baby hamster kidney (BHK) cell-derived clone constitutively expressing T7 RNA polymerase (20) (kindly provided by M. Sugiyama and N. Ito), has been shown to be highly potent for initiating the replication cycles of other negative-strand RNA viruses from cloned cDNAs (20, 48). By the use of previously reported methods of studies employing BHK/T7-9 cells (48), the cDNAs of the N, P, and L genes of MV were inserted into the pCITE vector; the resulting plasmids were termed pCITE-IC-N, pCITE-IC-PΔC, and pCITEko-9301B-L, respectively. These plasmids were designed to create an internal ribosome entry site at the 5′ terminus of the N, P, and L mRNAs. Since the ratios of the plasmids expressing the N, P, and L proteins were previously reported to be critical for the initiation of infectious cycles of paramyxoviruses from cloned cDNAs (13, 21, 26), the optimal ratio for these plasmids was determined using a minireplicon assay for MV (23). The analyses indicated that 0.20, 0.15, and 0.40 μg of pCITE-IC-N, pCITE-IC-PΔC, and pCITEko-9301B-L, respectively, were optimal for the expression of the MV minireplicon gene (luciferase) in BHK/T7-9 cells cultured in a 24-well cluster plate (see Table S3 in the supplemental material). When BHK/T7-9 cells cultured in a 6-well cluster plate were transfected with 5.0 μg of pHHRz-SI-AcGFP together with three support plasmids (0.80, 0.60, and 1.60 μg of pCITE-IC-N, pCITE-IC-PΔC, and pCITEko-9301B-L, respectively), infectious cycles of rSI-AcGFP were efficiently initiated from pHHRz-SI-AcGFP. Subsequently, the recombinant SI strain expressing AcGFP

TABLE 3. Detection of the M protein by an indirect immunofluorescence assay

MAb clone no.	Antigenic site	Assay result			
		IC323-AcGFP	SI-AcGFP	IC-M–mCherry	SI-M–mCherry
A23	II	+	−	+	−
A24	II	+	−	+	−
A27	II	+	−	+	−
A154	II	+	−	+	−
A157	II	+	−	+	−
A177	II	+	−	+	−
B46	II	+	−	+	−
A39	III	+	−	+	−
A41	III	+	−	+	−
A42	III	+	−	+	−
A51	III	+	−	+	−
A133	IV	+	−	+	−

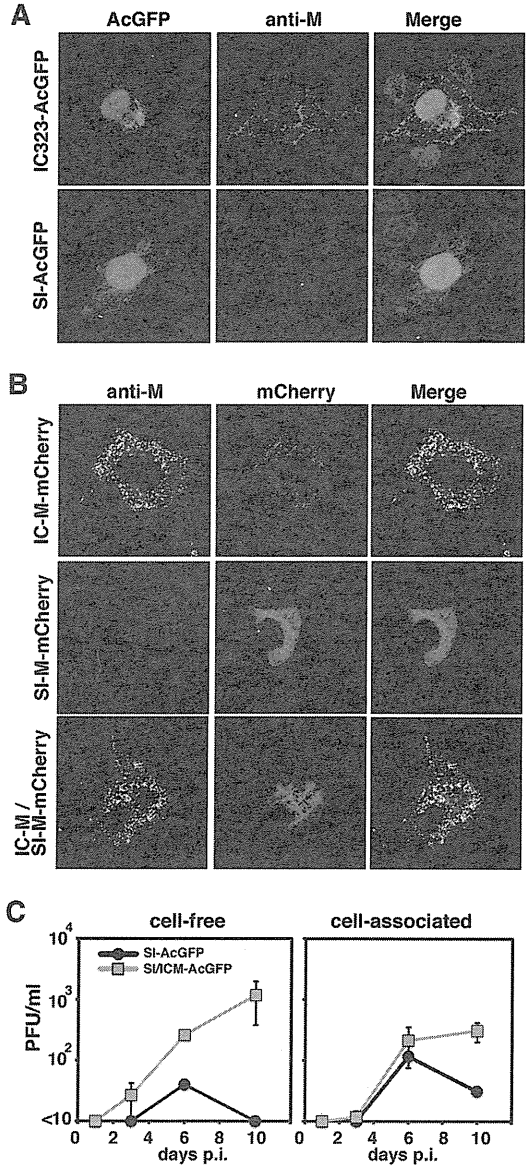

FIG. 3. Distribution of the M protein and effect on viral growth of strain SI possessing the IC-M gene. (A) Distribution of the M protein in cells infected with recombinant MV. Vero/hSLAM cells were infected with IC323-AcGFP or SI-AcGFP. At 2 (IC323-AcGFP) or 5 (SI-AcGFP) days postinfection, the cells were stained with an anti-M protein MAb (A42) and an Alexa Fluor 594-conjugated anti-mouse secondary antibody. The nuclei were stained with DAPI (blue). (B) Distribution of the mCherry-fused M protein. Vero/hSLAM cells were transfected with the M protein-expressing plasmids IC-M-mCherry, SI-M-mCherry, and IC-M plus SI-M-mCherry. At 1 day posttransfection, the cells were stained with an anti-M protein MAb (A42) and an Alexa 488-conjugated anti-mouse secondary antibody. The cells were observed under a confocal microscope. (C) Replication kinetics of recombinant MVs. Vero/hSLAM cells were infected with recombinant MVs at an MOI of 0.01, and infectious titers in culture medium (cell-free) and cells (cell-associated) were determined at 1, 3, 6, and 10 days p.i. Data represent the means ± standard deviations (SD) of results from triplicate samples.

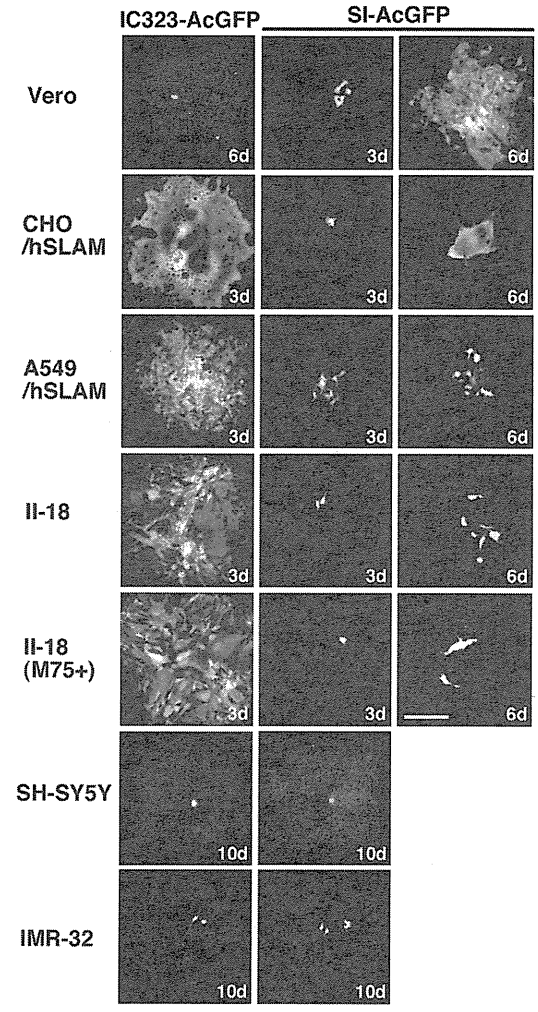

FIG. 4. AcGFP autofluorescence in cells infected with IC323-AcGFP and SI-AcGFP. Vero, CHO/hSLAM, A549/hSLAM, II-18, SH-SY5Y, and IMR-32 cells were infected with IC323-AcGFP or SI-AcGFP. Some II-18 cells were incubated with an anti-CD46 MAb (M75). The cells were observed under a fluorescence microscope at the indicated days (d). Bar, 0.20 mm.

(rSI-AcGFP) was maintained in Vero/hSLAM cells cocultured with BHK/T7-9 cells.

Properties of the M protein of the SI strain. Using various MAbs against the M protein (42), an indirect immunofluorescence assay was performed. A total of 12 MAbs that have been shown to recognize antigenic sites II, III, and IV of the M protein were used (42) (Table 3). A recombinant IC323 strain expressing AcGFP (IC323-AcGFP) was generated and used as a control. The IC323 strain is a recombinant MV based on the wt IC-B strain (60). In cells infected with IC323-AcGFP, all the MAbs detected the M protein (Fig. 3A and Table 3). However, in cells infected with the SI or rSI-AcGFP strains, all the MAbs failed to detect the M protein (Fig. 3A and Table 3 and data not shown). These data suggested a lack of M protein expression in cells infected with the SI and rSI-AcGFP strains. Sato et al. (43) also previously showed that M protein expression

TABLE 4. Amino acid substitutions in the H proteins of the IC, SI, and Edmonston strains

Amino acid no.	Amino acid substitution		
	IC	SI[a]	Ed[b]
7	R	Q*	R
71	H	R*	H
174	A	A	T
176	A	A	T
211	S	S	G
235	G	E	E
243	G	G	R
252	H	H	Y
276	F	F	L
284	F	F	L
296	F	F	L
302	R	R	G
334	R	Q	Q
390	N	M*	I
416	N	N	D
446	T	S	S
481	N	N	Y
482	L	F*	L
484	T	T	N
546	S	G*	S
555	F	L*	F
564	I	L*	I
575	K	Q	Q
600	V	V	E

[a] Asterisks indicate amino acids unique to the SI strain.
[b] Edmonston strain; GenBank accession number K01711.

was missing in cells infected with the SI strain. The M proteins of the SI and IC-B strains were expressed in cells by the use of expression plasmids. The carboxyl termini of the M proteins were tagged with mCherry red fluorescent protein. All the MAbs detected the IC-B strain-derived M protein despite the mCherry tag (Table 3). In contrast, none of the MAbs detected the SI strain-derived M protein, although bright mCherry fluorescence was detected in these cells (Fig. 3B and Table 3). These data indicated that the antigenicity of the M protein of the SI strain was totally different from that of the M protein of the IC-B strain and that none of the MAbs recognizing antigenic sites II, III, and IV reacted with the M protein of the SI strain. Therefore, we could not reach a conclusion as to whether the M protein was expressed in cells infected with the SI strain. However, analyses using the expression plasmids demonstrated that, unlike the M protein of the IC-B strain, the M protein of the SI strain was distributed homogeneously in cells (Fig. 3B). The M protein of the IC-B strain was distributed beneath the plasma membrane and formed small dots in the cytoplasm (Fig. 3B). To elucidate the functional difference between the IC-B and SI strains with respect to the M gene, we generated a recombinant MV with a modified SI strain genome in which the M gene was replaced with the M gene of the IC-B strain. The resulting recombinant MV was designated SI/ICM-AcGFP. A growth kinetics analysis showed that, unlike SI-AcGFP, SI/ICM-AcGFP produced cell-free virus well and the cell-free virus titer of SI/ICM-AcGFP was ~1,000 times higher than that of the SI-AcGFP at 10 days p.i. (Fig. 3C). The result demonstrated that SI-M protein was less involved in the budding stage. With these data, we concluded that the SI strain does not express a functional M protein.

The SI strain exhibits limited syncytium-forming activity. Various types of cells were infected with SI-AcGFP and IC323-AcGFP. IC323-AcGFP poorly entered Vero cells (SLAM$^-$/CD46$^+$) and did not produce a syncytium (Fig. 4). On the other hand, SI-AcGFP was able to produce syncytia in Vero cells (Fig. 4). Table 4 shows the amino acid substitutions in the H protein. Among them, the S546G substitution is the one that probably contributed to the ability of SI-AcGFP to produce syncytia in Vero cells, because this mutation allows MV to use CD46 as a receptor (69). On the other hand, SI-AcGFP failed to produce syncytia in II-18 cells (ECR$^+$, CD46$^+$), although IC323-AcGFP replicated and produced syncytia in these cells efficiently (Fig. 4). An MAb against CD46 (M75) had a neutral effect on the SI-AcGFP infection of II-18 cells. Similar results were obtained for the infection of SLAM-positive cells (CHO/hSLAM, A549/hSLAM). SI-AcGFP produced syncytia poorly in these cells, whereas IC323-AcGFP produced syncytia very efficiently. These data demonstrate that the SI strain has limited activity in inducing syncytia in SLAM- or ECR-expressing cells, although it has acquired the ability to use CD46 as an alternative receptor. Although three neural cell lines (SK-N-SH, IMR-32, and SH-SY5Y) were infected with SI-AcGFP and IC323-AcGFP, no syncytia were observed in these cells (Fig. 4 and data not shown).

The membrane-associated protein genes (M, F, and H) determine the growth phenotype of the SI strain. The amino acid sequences of the RNP component proteins (N, P, and L pro-

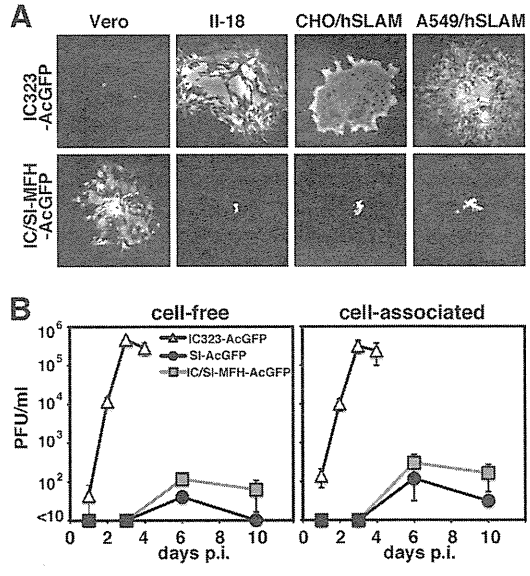

FIG. 5. Effect on viral growth of strain IC possessing the SI-MFH gene in various cell lines. (A) AcGFP fluorescence in cells infected with recombinant MVs. Vero, II-18, CHO/hSLAM, and A549/hSLAM cells were infected with IC323-AcGFP or IC323/SI-MFH-AcGFP. The cells were observed under a fluorescence microscope at 3 (II-18, CHO/hSLAM, and A549/hSLAM) and 6 (Vero) days postinfection. (B) Replication kinetics of recombinant MVs. Vero/hSLAM cells were infected with recombinant MVs at an MOI of 0.01. At various time intervals, infectious titers in culture medium (cell-free) and cells (cell-associated) were determined. Data represent the means ± standard deviations (SD) of the results of experiments performed with triplicate samples.

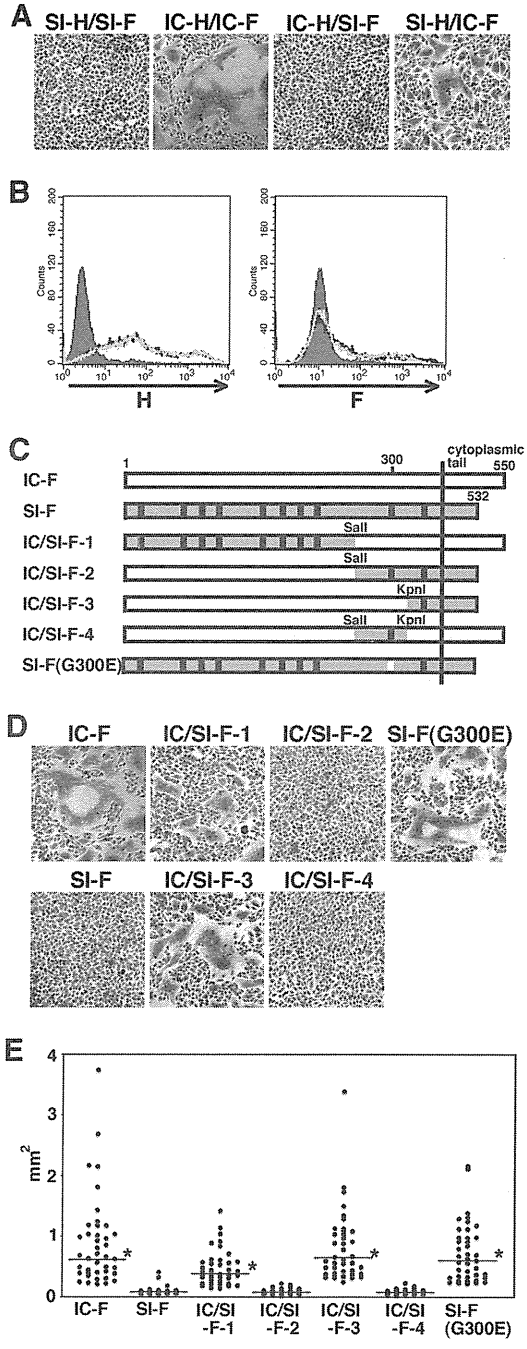

FIG. 6. Syncytium formation in cells expressing H and F proteins and identification of the amino acid residue in the F protein of the SI strain critical for reducing cell-to-cell fusion. (A) Syncytium formation in cells expressing H and F proteins of the IC-B or SI strains. CHO/hSLAM cells were transfected with a plasmid expressing the H protein of the IC-B or SI strain (IC-H or SI-H, respectively) together with a plasmid expressing the F protein of the IC-B or SI strain (IC-F or SI-F, respectively). At 24 h posttransfection, the cells were observed under a microscope after Giemsa staining. (B) Expression of the MV envelope proteins on the cells. CHO/hSLAM cells were transfected with a plasmid expressing IC-H, SI-H, IC-F, or SI-F. The cells expressing IC-H (black line) and SI-H (gray line) were stained with an anti-H protein MAb (left panel), and the cells expressing IC-F (black line) and SI-F (gray line) were stained with an anti-F protein MAb (right panel). All the cells were subsequently stained with an Alexa Fluor 488-conjugated secondary antibody. The cells without transfection were stained with an anti-H protein MAb or an anti-F protein MAb followed by an Alexa Fluor 488-conjugated secondary antibody (shaded regions). (C) Diagrams of the chimeric F proteins. There are 10 amino acid differences (shown by vertical lines) between IC-F and SI-F. The regions derived from SI-F are shaded, and those derived from IC-F are white. The restriction enzyme-replaced fragments are indicated. (D) Syncytium formation in cells expressing the chimeric or mutant F proteins. CHO/hSLAM cells were transfected with a plasmid expressing IC-H together with plasmids expressing IC-F protein, SI-F protein, chimeric F protein (IC/SI-F-1, -F-2, -F-3, or -F-4), or mutant SI-F protein (G300E). At 24 h posttransfection, the cells were observed under a phase-contrast imaging microscope after Giemsa staining. (E) Quantification of syncytium formation. CHO/hSLAM cells were transfected with IC-H-expressing plasmids and IC-F-, SI-F-, chimeric F-, or mutant F-expressing plasmids together with an mCherry-expressing plasmid. At 48 h posttransfection, areas of each syncytium with mCherry autofluorescence were measured using an Axio Observer.D1 microscope and ImageJ software. Forty syncytia were measured for each F protein. Asterisks indicate that the area of syncytia induced by IC-F, chimeric F, or mutant F was significantly larger than that induced by SI-F, based on the results of a t test ($P < 0.001$). The horizontal bars indicate the median values of the areas of syncytia.

teins) and nonstructural C and V proteins were well conserved in the SI strain (Table 1). We generated a recombinant MV possessing the IC323 genome in which the M, F, and H genes were replaced with those of the SI strain. The recombinant MV was designated IC/SI-MFH-AcGFP. The various types of cells shown in Fig. 4 were infected with IC/SI-MFH-AcGFP. IC/SI-MFH-AcGFP replicated poorly in SLAM- and ECR-positive cells and did not produce syncytia in these cells (Fig. 5A). A growth kinetics analysis of Vero/hSLAM cells, which were susceptible to all recombinant MVs, showed that IC/SI-MFH-AcGFP hardly produced cell-free viruses and exhibited a growth phenotype similar to that of SI-AcGFP (Fig. 4 and 5B). These data indicated that the membrane-associated protein-encoding genes (i.e., the M, F, and H genes) were responsible for the growth phenotype of the SI strain.

The E300G substitution in the F protein is responsible for the reduced membrane fusion activity. Previous papers have indicated that the typical changes in SSPE strains, namely, the lack of M protein expression and cytoplasmic tail truncation of the F protein, enhance the syncytium-forming activity of MV (6, 7). Indeed, other previous papers have shown high fusogenic activities of SSPE strains (1, 4, 8). Despite exhibiting the changes typical in SSPE strains, SI-AcGFP and IC/SI-MFH-AcGFP showed limited syncytium-forming activities (Fig. 4 and 5B). Using expression plasmids, the syncytium-forming activities of the H and F proteins of the SI strain were analyzed in CHO/hSLAM cells ($SLAM^+$). When the F protein of the SI strain (SI-F) was expressed together with the H protein of the SI strain (SI-H), no syncytia were detected (Fig. 6A; SI-H/SI-F). In contrast, many syncytia were observed when the F and H proteins of the IC-B strain (IC-F and IC-H, respectively) were expressed (Fig. 6A; IC-H/IC-F). Flow cytometry analyses indicated that the expression levels of SI-F and SI-H, respectively, were similar to those of IC-F and IC-H (Fig. 6B). The combination of SI-F and IC-H also showed poor syncytium-forming activity (Fig. 6A; IC-H/SI-F). On the other hand, when IC-F

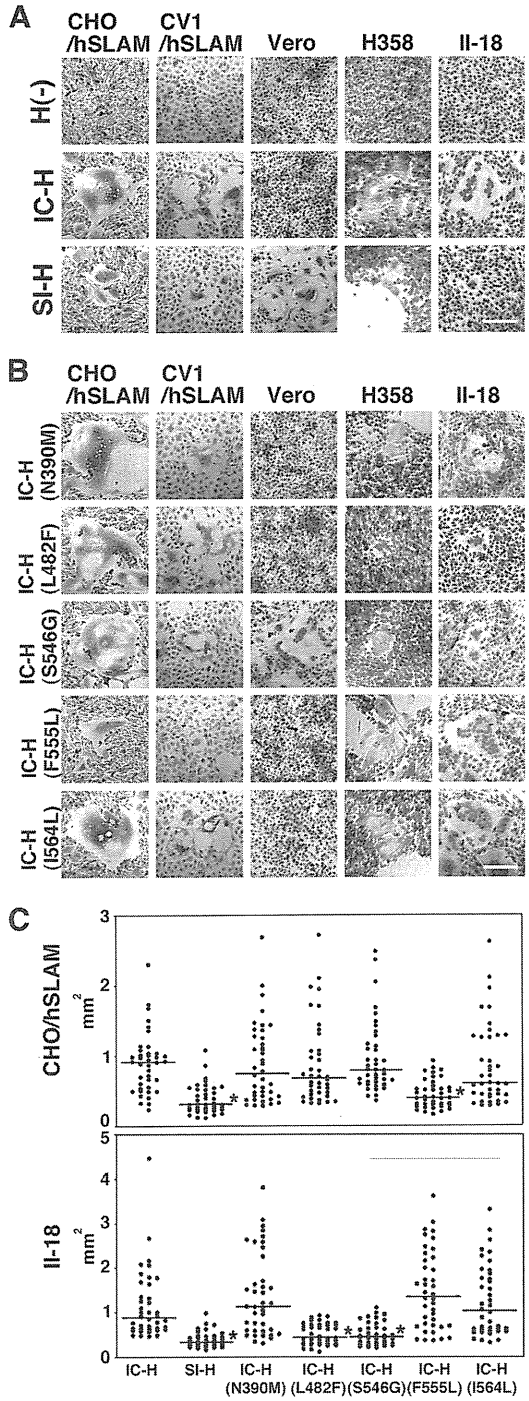

FIG. 7. Characterization of the amino acid residues in the SI-H protein that support cell-to-cell fusion in cells expressing SLAM, CD46, or ECR. (A and B) CHO/hSLAM, CV1/hSLAM, Vero, H358, and II-18 cells were transfected with plasmids expressing the H protein of the IC-B or SI strain (IC-H or SI-H, respectively) or no H protein [H(−)] (A) or mutant IC-H protein (N390M, L482F, S546G, F555L, or I564L) (B) together with a plasmid expressing the F protein of the IC-B strain. The CV1/hSLAM, H358, and II-18 cells were then incubated with an anti-CD46 MAb (M75). At 1 (CHO/hSLAM and CV1/hSLAM), 2 (Vero and II-18), or 3 (H358) days posttransfection, the cells were observed under a phase-contrast imaging microscope after Giemsa staining. Bars, 0.2 mm. (C) Quantification of syncytium formation. CHO/hSLAM and II-18 cells were transfected with IC-F-expressing plasmids and IC-H-, SI-H-, or mutant H-expressing plasmids together with an mCherry-expressing plasmid. At 48 h posttransfection, areas of each syncytium with mCherry autoflurescence were measured using an Axio Observer.D1 microscope and ImageJ software. Forty syncytia were measured for each H protein. Asterisks indicate that the area of syncytia induced by SI-H or mutant H was significantly smaller than that induced by the IC-H, based on the results of a t test ($P < 0.001$). The horizontal bars indicate the median values of the areas of syncytia.

was coexpressed with SI-H, many syncytia, albeit smaller in size than the syncytia induced by IC-F and IC-H, were detected (Fig. 6A; SI-H/IC-F). These data indicated that both the SI-F and SI-H proteins exhibited lower activities than the IC-F and IC-H proteins in inducing syncytia in CHO/hSLAM cells. To identify the mutation(s) that impaired the syncytium-forming activity of SI-F, four chimeric F proteins (IC/SI-F-1, -F-2, -F-3, and -F-4) were generated using the SI and IC-B strains (Fig. 6C). These chimeric F proteins were coexpressed with IC-H. Two chimeric F proteins, IC/SI-F-2 and IC/SI-F-4, failed to produce syncytia (Fig. 6D and E). These data showed that a region between the SalI and KpnI recognition sites (amino acid positions 271 and 324) in SI-F severely restricted its membrane fusion activity (Fig. 6C). In this region, only a single amino acid substitution, E300G, was found in comparisons of SI-F and IC-F (Fig. 6C and Table 2). A glycine residue at amino acid position 300 in SI-F was replaced with a glutamic acid. The mutant F protein [Fig. 6C; SI-F(G300E)] was expressed with IC-H. The data indicated that SI-F(G300E) caused membrane fusion as well as IC-F did ($P < 0.01$) [Fig. 6D and E; SI-F(G300E)]. These findings indicated that the SI-F protein exhibited a restricted membrane fusion activity that was mainly caused by the E300G substitution.

S546G, L482F, and F555L substitutions affected the fusion-helper function of the H protein. To analyze the fusion-helper function of SI-H in different cell types, the protein was expressed in CHO/hSLAM ($SLAM^+$), CV1/hSLAM ($SLAM^+$, $CD46^+$), Vero ($CD46^+$), H358 (ECR^+, $CD46^+$), and II-18 (ECR^+, $CD46^+$) cells together with IC-F. CD46-dependent infection was blocked by an anti-CD46 antibody (M75) when CV1/hSLAM, H358, and II-18 cells were used for the assessment of SLAM- and ECR-dependent infection. IC-H was used as a control. When IC-F was expressed alone, no syncytia were observed in either cell line [Fig. 7A; H(−)]. As reported previously, IC-H supported cell-to-cell fusion efficiently in SLAM-positive (CHO/hSLAM) and ECR-positive (H358 and II-18) cells but not in Vero cells (Fig. 7A; IC-H) (45, 49, 59). SI-H exhibited a fusion-helper function in Vero cells (Fig. 7A; SI-H), probably because of the S546G substitution. However, SI-H supported cell-to-cell fusion less efficiently than IC-H in CHO/hSLAM, CV1/hSLAM, H358, and II-18 cells (Fig. 7A; SI-H). To identify the substitution(s) responsible for the altered fusion-helper function of SI-H, five substitutions were individually introduced into IC-H and the mutated proteins were expressed in cells together with IC-F. The five selected substitutions were N390M, L482F, S546G, F555L, and 564L, since these substitutions were unique to the SI strain and

located in the receptor-binding globular head domain (Table 4). As expected, IC-H with S546G, but not the other mutant H proteins, supported cell-to-cell fusion in Vero cells (Fig. 7B). Instead, IC-H with S546G showed a reduced fusion-helper function in H358 and II-18 cells (Fig. 7B). No significant changes were observed in CHO/hSLAM and CV1/hSLAM cells after the introduction of the S546G substitution (Fig. 7B). Similarly, IC-H with L482F showed a reduced fusion-helper function in H358 and II-18 cells but showed activities similar to those seen with IC-H in CHO/hSLAM and CV1/hSLAM cells (Fig. 7B). Quantified and statistical analyses of cell-to-cell fusion in II-18 cells indicated that the areas of syncytia produced by IC-H(S546G) and IC-H(L482F) were significantly smaller than those produced by IC-H ($P < 0.01$) (Fig. 7C). None of the N390M, F555L, and I564L substitutions significantly affected the fusion-helper function in H358 and II-18 cells (Fig. 7B and C). These findings suggested that the L482F and S546G substitutions compromised the ability of the H protein to interact with ECR. It was also noted that the H protein with F555L showed a reduction in the fusion-helper function in CHO/hSLAM and CV1/hSLAM cells (Fig. 7B and C).

DISCUSSION

SLAM is expressed on cells of the immune system and functions as the principal receptor for MV infection (69). However, this molecule probably plays a minor role in MV growth in the CNS, because neural cells in the brain do not express SLAM (28). Indeed, the ability of the SI strain to use SLAM was compromised by the F555L substitution. We and another group recently demonstrated that certain epithelial cells that form tight junctions are highly susceptible to MV infection (25, 50, 59). These data demonstrated the existence of ECR on some epithelial cells (25, 50, 59). ECR probably contributes to the efficient transmission of MV from a patient to other individuals (53), but its roles in persistent infection of the brain with MV remain to be elucidated. ECR is a candidate for an MV receptor in the brain. However, our data indicated that the SI strain had mutated via the S546G and L482F substitutions to use ECR inefficiently. With these data, the idea that ECR functions as a receptor for MV in the brain seemed unconvincing. Instead, the SI-H protein had adapted to use CD46 via the S546G substitution. Woelk et al. identified several positive-selection amino acid sites in the SSPE strain (67), but S546G was absent from the list. It is possible that the S546G substitution was introduced into the SI strain genome during the propagation in Vero cells but not in the brain, since the SI strain was isolated using Vero cells (29). Vero cells are 100 to 1,000 times less sensitive than SLAM-positive B95a cells for the isolation of wt MV strains (22, 34), and wt MV strains readily adapt to use CD46 after several passages in Vero cells (69). However, Ogura et al. (34) indicated that Vero cells were more sensitive than B95a cells for the isolation of SSPE strains. Although their data demonstrated that SSPE strains show cell specificities different from those of wt MV strains, some SSPE strains were shown not to use CD46 as a receptor (47). Nevertheless, it is still possible that the acquisition of the ability to use CD46 contributes to the growth of some SSPE-derived strains in the brain, since various SSPE strains may employ different strategies to acquire the ability to spread in the brain. The SI strain used only CD46 efficiently. Much evidence obtained using CD46-transgenic mice has shown the contributions of CD46 in establishing MV infection of the brain. Analyses using human brain samples also showed that CD46 is a candidate molecule that contributes to the growth of some SSPE strains in the brain (5, 28, 33).

Analyses using animal models have demonstrated that MV uses a transsynaptic route to spread between neurons (24, 27, 35, 40). The data indicated that receptors for the H protein are not required for the transsynaptic transmission (27, 70). It has been suggested that the F protein causes microfusion between neurons without the support of the H protein (27, 70). Ayata et al. (1) demonstrated that the F proteins of some SSPE strains contribute to the exhibition of neurovirulence in animals by showing a hyperfusion activity. Cattaneo et al. (4, 8) also demonstrated that the F proteins of SSPE strains exhibit higher levels of fusion activities than the standard F protein. These data suggest an important role for the F protein in the propagation of SSPE strains in the brain. However, our data indicated that the F protein of the SI strain showed limited membrane fusion activity because of the E300G substitution. It is unlikely that the F protein of the SI strain had acquired the E300G substitution during the propagation in cultured cells, since viruses usually acquire mutations that confer better fitness. Consequently, our data suggest that a high level of membrane fusion activity of the F protein was not a prerequisite for this SSPE strain to spread in the brain. Watanabe et al. (65) suggested that a reduction in cell-to-cell fusion mediated by amino acid changes in the F protein contributes to the persistence of MV in the brain. Their observations are consistent with our data for the SI strain. Thus, the data obtained in the present study provide a clear example of an SSPE-derived strain that exhibits limited fusion activity.

In the present study, we also established a reverse genetics system for the SI strain. Although we previously reported very efficient reverse genetics systems for MV, as shown using recombinant vaccinia viruses encoding T7 RNA polymerase (VV-T7) (30, 55, 56), they were not applicable for rescue of the SI strain from cloned cDNAs. When the previous systems were used (30, 56), infectious cycles of rSI-AcGFP were efficiently initiated in CHO/hSLAM cells by the use of the full-length genome plasmid (data not shown). However, since rSI-AcGFP did not produce cell-free virus particles and replicated poorly, it was impossible to isolate rSI-AcGFP from VV-T7. We tried to use a VV-T7-free system reported by Radecke et al. (39), but neither syncytia nor AcGFP fluorescence was detected. Therefore, a new, efficient VV-T7-free system was required for the rescue of rSI-AcGFP from cloned cDNAs. We are convinced that this new system used for the SI strain would be applicable for other SSPE strains. The success in establishing a reverse genetics system for an SSPE strain is a significant step toward the elucidation of the molecular bases and pathogenesis of SSPE.

ACKNOWLEDGMENTS

We thank T. A. Sato and T. Seya for providing MAbs and N. Ito and M. Sugiyama for providing the BHK/T7-9 cells. We also thank K. Maenaka and all the members of Department of Virology 3, NIID, Japan, for technical help and suggestions.

This work was supported by grants from the Ministry of Education, Culture, Sports, Science and Technology and the Ministry of Health,

Labor and Welfare of Japan and a grant from The Uehara Memorial Foundation.

REFERENCES

1. **Ayata, M., et al.** 2007. Effect of the alterations in the fusion protein of measles virus isolated from brains of patients with subacute sclerosing panencephalitis on syncytium formation. Virus Res. **130:**260–268.
2. **Baricevic, M., D. Forcic, M. Santak, and R. Mazuran.** 2007. A comparison of complete untranslated regions of measles virus genomes derived from wild-type viruses and SSPE brain tissues. Virus Genes **35:**17–27.
3. **Bellini, W. J., et al.** 2005. Subacute sclerosing panencephalitis: more cases of this fatal disease are prevented by measles immunization than was previously recognized. J. Infect. Dis. **192:**1686–1693.
4. **Billeter, M. A., et al.** 1994. Generation and properties of measles virus mutations typically associated with subacute sclerosing panencephalitis. Ann. N. Y. Acad. Sci. **724:**367–377.
5. **Buchholz, C. J., et al.** 1996. Selective expression of a subset of measles virus receptor-competent CD46 isoforms in human brain. Virology **217:**349–355.
6. **Cathomen, T., et al.** 1998. A matrix-less measles virus is infectious and elicits extensive cell fusion: consequences for propagation in the brain. EMBO J. **17:**3899–3908.
7. **Cathomen, T., H. Y. Naim, and R. Cattaneo.** 1998. Measles viruses with altered envelope protein cytoplasmic tails gain cell fusion competence. J. Virol. **72:**1224–1234.
8. **Cattaneo, R., and J. K. Rose.** 1993. Cell fusion by the envelope glycoproteins of persistent measles viruses which caused lethal human brain disease. J. Virol. **67:**1493–1502.
9. **Cattaneo, R., et al.** 1988. Biased hypermutation and other genetic changes in defective measles viruses in human brain infections. Cell **55:**255–265.
10. **Cattaneo, R., et al.** 1986. Accumulated measles virus mutations in a case of subacute sclerosing panencephalitis: interrupted matrix protein reading frame and transcription alteration. Virology **154:**97–107.
11. **Cattaneo, R., et al.** 1989. Mutated and hypermutated genes of persistent measles viruses which caused lethal human brain diseases. Virology **173:**415–425.
12. **Griffin, D. E.** 2007. Measles virus, p. 1551–1585. *In* D. M. Knipe et al. (ed.), Fields virology, 5th ed. Lippincott Williams & Wilkins, Philadelphia, PA.
13. **Grosfeld, H., M. G. Hill, and P. L. Collins.** 1995. RNA replication by respiratory syncytial virus (RSV) is directed by the N, P, and L proteins; transcription also occurs under these conditions but requires RSV superinfection for efficient synthesis of full-length mRNA. J. Virol. **69:**5677–5686.
14. **Hall, W. W., and P. W. Choppin.** 1979. Evidence for lack of synthesis of the M polypeptide of measles virus in brain cells in subacute sclerosing panencephalitis. Virology **99:**443–447.
15. **Hall, W. W., and P. W. Choppin.** 1981. Measles-virus proteins in the brain tissue of patients with subacute sclerosing panencephalitis: absence of the M protein. N. Engl. J. Med. **304:**1152–1155.
16. **Hall, W. W., R. A. Lamb, and P. W. Choppin.** 1979. Measles and subacute sclerosing panencephalitis virus proteins: lack of antibodies to the M protein in patients with subacute sclerosing panencephalitis. Proc. Natl. Acad. Sci. U. S. A. **76:**2047–2051.
17. **Halsey, N. A., et al.** 1980. Risk factors in subacute sclerosing panencephalitis: a case-control study. Am. J. Epidemiol. **111:**415–424.
18. **Hirano, A., A. H. Wang, A. F. Gombart, and T. C. Wong.** 1992. The matrix proteins of neurovirulent subacute sclerosing panencephalitis virus and its acute measles virus progenitor are functionally different. Proc. Natl. Acad. Sci. U. S. A. **89:**8745–8749.
19. **Ishida, H., et al.** 2004. Infection of different cell lines of neural origin with subacute sclerosing panencephalitis (SSPE) virus. Microbiol. Immunol. **48:**277–287.
20. **Ito, N., et al.** 2003. Improved recovery of rabies virus from cloned cDNA using a vaccinia virus-free reverse genetics system. Microbiol. Immunol. **47:**613–617.
21. **Kato, A., et al.** 1996. Initiation of Sendai virus multiplication from transfected cDNA or RNA with negative or positive sense. Genes Cells **1:**569–579.
22. **Kobune, F., H. Sakata, and A. Sugiura.** 1990. Marmoset lymphoblastoid cells as a sensitive host for isolation of measles virus. J. Virol. **64:**700–705.
23. **Komase, K., et al.** 2006. The phosphoprotein of attenuated measles AIK-C vaccine strain contributes to its temperature-sensitive phenotype. Vaccine **24:**826–834.
24. **Lawrence, D. M., et al.** 2000. Measles virus spread between neurons requires cell contact but not CD46 expression, syncytium formation, or extracellular virus production. J. Virol. **74:**1908–1918.
25. **Leonard, V. H., et al.** 2008. Measles virus blind to its epithelial cell receptor remains virulent in rhesus monkeys but cannot cross the airway epithelium and is not shed. J. Clin. Invest. **118:**2448–2458.
26. **Leyrer, S., W. J. Neubert, and R. Sedlmeier.** 1998. Rapid and efficient recovery of Sendai virus from cDNA: factors influencing recombinant virus rescue. J. Virol. Methods **75:**47–58.
27. **Makhortova, N. R., et al.** 2007. Neurokinin-1 enables measles virus trans-synaptic spread in neurons. Virology **362:**235–244.
28. **McQuaid, S., and S. L. Cosby.** 2002. An immunohistochemical study of the distribution of the measles virus receptors, CD46 and SLAM, in normal human tissues and subacute sclerosing panencephalitis. Lab. Invest. **82:**403–409.
29. **Mirchamsy, H., et al.** 1978. Isolation and characterization of a defective measles virus from brain biopsies of three patients in Iran with subacute sclerosing panencephalitis. Intervirology **9:**106–118.
30. **Nakatsu, Y., M. Takeda, M. Kidokoro, M. Kohara, and Y. Yanagi.** 2006. Rescue system for measles virus from cloned cDNA driven by vaccinia virus Lister vaccine strain. J. Virol. Methods **137:**152–155.
31. **Ning, X., et al.** 2002. Alterations and diversity in the cytoplasmic tail of the fusion protein of subacute sclerosing panencephalitis virus strains isolated in Osaka, Japan. Virus Res. **86:**123–131.
32. **Niwa, H., K. Yamamura, and J. Miyazaki.** 1991. Efficient selection for high-expression transfectants with a novel eukaryotic vector. Gene **108:**193–199.
33. **Ogata, A., et al.** 1997. Absence of measles virus receptor (CD46) in lesions of subacute sclerosing panencephalitis brains. Acta Neuropathol. **94:**444–449.
34. **Ogura, H., et al.** 1997. Efficient isolation of subacute sclerosing panencephalitis virus from patient brains by reference to magnetic resonance and computed tomographic images. J. Neurovirol. **3:**304–309.
35. **Oldstone, M. B. A., et al.** 1999. Measles virus infection in a transgenic model: virus-induced immunosuppression and central nervous system disease. Cell **98:**629–640.
36. **Ono, N., et al.** 2001. Measles viruses on throat swabs from measles patients use signaling lymphocytic activation molecule (CDw150) but not CD46 as a cellular receptor. J. Virol. **75:**4399–4401.
37. **Parks, C. L., et al.** 2001. Comparison of predicted amino acid sequences of measles virus strains in the Edmonston vaccine lineage. J. Virol. **75:**910–920.
38. **Radecke, F., and M. A. Billeter.** 1995. Appendix: measles virus antigenome and protein consensus sequences. Curr. Top. Microbiol. Immunol. **191:**181–192.
39. **Radecke, F., et al.** 1995. Rescue of measles viruses from cloned DNA. EMBO J. **14:**5773–5784.
40. **Rall, G. F., et al.** 1997. A transgenic mouse model for measles virus infection of the brain. Proc. Natl. Acad. Sci. U. S. A. **94:**4659–4663.
41. **Richardson, C. D., A. Scheid, and P. W. Choppin.** 1980. Specific inhibition of paramyxovirus and myxovirus replication by oligopeptides with amino acid sequences similar to those at the N-termini of the F1 or HA2 viral polypeptides. Virology **105:**205–222.
42. **Sato, T. A., A. Fukuda, and A. Sugiura.** 1985. Characterization of major structural proteins of measles virus with monoclonal antibodies. J. Gen. Virol. **66:**1397–1409.
43. **Sato, T. A., M. Hayami, and K. Yamanouchi.** 1981. Antibody response to structural proteins of measles virus in patients with natural measles and subacute sclerosing panencephalitis. Jpn. J. Med. Sci. Biol. **34:**365–373.
44. **Schmid, A., et al.** 1992. Subacute sclerosing panencephalitis is typically characterized by alterations in the fusion protein cytoplasmic domain of the persisting measles virus. Virology **188:**910–915.
45. **Seki, F., M. Takeda, H. Minagawa, and Y. Yanagi.** 2006. Recombinant wild-type measles virus containing a single N481Y substitution in its haemagglutinin cannot use receptor CD46 as efficiently as that having the haemagglutinin of the Edmonston laboratory strain. J. Gen. Virol. **87:**1643–1648.
46. **Seya, T., et al.** 1995. Blocking measles virus infection with a recombinant soluble from of, or monoclonal antibodies against, membrane cofactor protein of complement (CD46). Immunology **84:**619–625.
47. **Shingai, M., et al.** 2003. Receptor use by vesicular stomatitis virus pseudotypes with glycoproteins of defective variants of measles virus isolated from brains of patients with subacute sclerosing panencephalitis. J. Gen. Virol. **84:**2133–2143.
48. **Shirogane, Y., et al.** 2008. Efficient multiplication of human metapneumovirus in Vero cells expressing the transmembrane serine protease TMPRSS2. J. Virol. **82:**8942–8946.
49. **Shirogane, Y., et al.** 2010. Epithelial-mesenchymal transition abolishes the susceptibility of polarized epithelial cell lines to measles virus. J. Biol. Chem. **285:**20882–20890.
50. **Tahara, M., et al.** 2008. Measles virus infects both polarized epithelial and immune cells by using distinctive receptor-binding sites on its hemagglutinin. J. Virol. **82:**4630–4637.
51. **Tahara, M., M. Takeda, and Y. Yanagi.** 2005. Contributions of matrix and large protein genes of the measles virus Edmonston strain to growth in cultured cells as revealed by recombinant viruses. J. Virol. **79:**15218–15225.
52. **Takasu, T., et al.** 2003. A continuing high incidence of subacute sclerosing panencephalitis (SSPE) in the Eastern Highlands of Papua New Guinea. Epidemiol. Infect. **131:**887–898.
53. **Takeda, M.** 2008. Measles virus breaks through epithelial cell barriers to achieve transmission. J. Clin. Invest. **118:**2386–2389.
54. **Takeda, M., et al.** 1998. Measles virus attenuation associated with transcriptional impediment and a few amino acid changes in the polymerase and accessory proteins. J. Virol. **72:**8690–8696.

55. **Takeda, M., et al.** 2006. Generation of measles virus with a segmented RNA genome. J. Virol. **80:**4242–4248.
56. **Takeda, M., et al.** 2005. Efficient rescue of measles virus from cloned cDNA using SLAM-expressing Chinese hamster ovary cells. Virus Res. **108:**161–165.
57. **Takeda, M., et al.** 2005. Long untranslated regions of the measles virus M and F genes control virus replication and cytopathogenicity. J. Virol. **79:** 14346–14354.
58. **Takeda, M., et al.** 2008. Measles viruses possessing the polymerase protein genes of the Edmonston vaccine strain exhibit attenuated gene expression and growth in cultured cells and SLAM knock-in mice. J. Virol. **82:**11979–11984.
59. **Takeda, M., et al.** 2007. A human lung carcinoma cell line supports efficient measles virus growth and syncytium formation via a SLAM- and CD46-independent mechanism. J. Virol. **81:**12091–12096.
60. **Takeda, M., et al.** 2000. Recovery of pathogenic measles virus from cloned cDNA. J. Virol. **74:**6643–6647.
61. **Takeuchi, K., N. Miyajima, F. Kobune, and M. Tashiro.** 2000. Comparative nucleotide sequence analysis of the entire genomes of B95a cell-isolated and Vero cell-isolated measles viruses from the same patient. Virus Genes **20:** 253–257.
62. **Tatsuo, H., N. Ono, K. Tanaka, and Y. Yanagi.** 2000. SLAM (CDw150) is a cellular receptor for measles virus. Nature **406:**893–897.
63. **Thompson, J. D., D. G. Higgins, and T. J. Gibson.** 1994. CLUSTAL W: improving the sensitivity of progressive multiple sequence alignment through sequence weighting, position-specific gap penalties and weight matrix choice. Nucleic Acids Res. **22:**4673–4680.
64. **Wang, D., Y. Zhang, Z. Zhang, J. Zhu, and J. Yu.** 2010. KaKs_Calculator 2.0: a toolkit incorporating gamma-series methods and sliding window strategies. Genomics Proteomics Bioinformatics **8:**77–80.
65. **Watanabe, M., et al.** 1995. Delayed activation of altered fusion glycoprotein in a chronic measles virus variant that causes subacute sclerosing panencephalitis. J. Neurovirol. **1:**177–188.
66. **WHO.** 2003. Update of the nomenclature for describing the genetic characteristics of wild-type measles viruses: new genotypes and reference strains. Wkly. Epidemiol. Rec. **78:**229–232.
67. **Woelk, C. H., O. G. Pybus, L. Jin, D. W. Brown, and E. C. Holmes.** 2002. Increased positive selection pressure in persistent (SSPE) versus acute measles virus infections. J. Gen. Virol. **83:**1419–1430.
68. **Wong, T. C., et al.** 1989. Generalized and localized biased hypermutation affecting the matrix gene of a measles virus strain that causes subacute sclerosing panencephalitis. J. Virol. **63:**5464–5468.
69. **Yanagi, Y., M. Takeda, S. Ohno, and T. Hashiguchi.** 2009. Measles virus receptors. Curr. Top. Microbiol. Immunol. **329:**13–30.
70. **Young, V. A., and G. F. Rall.** 2009. Making it to the synapse: measles virus spread in and among neurons. Curr. Top. Microbiol. Immunol. **330:**3–30.

Vaccines & Vaccination

Piao et al. J Vaccines Vaccin 2011, 2:1
http://dx.doi.org/10.4172/2157-7560.1000113

Research Article Open Access

Comparative Effects of Toll-Like Receptor Agonists on a Low Dose PspA Intranasal Vaccine against Fatal Pneumococcal Pneumonia in Mice

Zhenyu Piao[1,2], Keita Oma[1,3], Hirokazu Ezoe[1], Yukihiro Akeda[1], Kazunori Tomono[2] and Kazunori Oishi[1]*

[1]*Laboratory for Clinical Research on Infectious Diseases, International Research Center for Infectious Diseases, Research Institute for Microbial Diseases, 3-1 Yamadaoka*
[2]*Division of Infection Control and Prevention, Osaka University Graduate School of Medicine, 2-15 Yamadaoka, Suita, Osaka 565-0871*
[3]*OK Pharmacy, Nagasaki, Nagasaki 850-0841, Japan*

Abstract

To develop a cost-effective pneumococcal vaccine, we compared the effects of a panel of Toll-like receptor (TLR) agonists on a low dose pneumococcal surface protein A (PspA) nasal vaccine in a fatal pneumococcal pneumonia model using a serotype 3 strain. The mice were nasally immunized with 10 μg of the TLR agonist (TLR 2, 3, 4 and 9) and 0.1μg of PspA once per week for three weeks. A high level of PspA-specific immunoglobulin G (IgG) was detected in sera of mice that were nasally administered a low dose of PspA plus each TLR agonist, while no PspA-specific IgG were detected in sera of mice that had been nasally administered a low dose of PspA alone. A relatively low level of PspA-specific IgG was also detected in the airway of mice that had been nasally administered a low dose of PspA plus each TLR agonist. The binding of PspA-specific IgG increased the deposition of C3 on the bacterial surface. Bacterial density in the lung and blood was significantly decreased in mice that had been administered a low dose of PspA plus each TLR agonist, compared with mice that received a low dose of PspA alone 24 h after a bacterial challenge. Furthermore, significant increases in survival rate were found in a murine model of fatal pneumonia that had been nasally administered a low dose of PspA plus each TLR agonist, compared with mice that received a low dose of PspA alone. The rank order of TLR agonists on the effect of increasing survival rate was LPS > Pam3CSK4 > Poly(I:C) and CpG 1826. These data suggest a potentially new strategy for the development of a cost-effective intranasal vaccine with a low dose PspA plus TLR agonist that would be effective against life-threatening bacteremic pneumococcal pneumonia.

Keywords: PspA; TLR agonist; Intranasal vaccine; *Streptococcus pneumoniae*; Pneumonia

Abbreviations: PspA: Pneumococcal surface protein A; TLR: Toll-Like Receptor; LPS: Lipopolysaccharide; Poly(I:C): Polyinosine-polycytidylic acid; CpG ODN 1826: CpG-Containing Oligodeoxynucleotide 1826; BALF: Bronchoalveolar lavage fluid; NW: Nasal wash

Introduction

S. pneumoniae is a leading human pathogen that causes a wide variety of diseases, ranging from otitis media to pneumonia, bacteremia, and meningitis in both children and adults. Pneumococcal infections can occur at any age but are more frequent in infants, the elderly and immunocompromised patients. Despite the development of effective treatments, the pneumococcus has remained a significant cause of morbidity and mortality worldwide [1,2]. Because of this, a clear need for an effective vaccine for the prevention of disease exists. Currently licensed polysaccharide-based pneumococcal vaccines only elicit protective antibodies against the infection of serotypes that are included in the vaccine. In addition, invasive diseases attributable to non-vaccine serotypes of *S. pneumoniae* have increased greatly [3,4]. Therefore, the search for new vaccine candidates that elicit protection against a broader range of pneumococcal strains is an important goal. To broaden the protection, the use of pneumococcal proteins represents a feasible and preferable alternative. Several pneumococcal proteins are currently under investigation as potential candidates for such a vaccine [5,6]. One of these proteins, PspA has recently undergone phase one clinical trials in humans and has been found to be safe and highly immunogenic [7,8]. PspA is a surface protein of *S. pneumoniae* that is found on all pneumococci and is broadly expressed among different serotypes of pneumococci [8]. Antibodies to PspA generated in mice [9,10] or humans [7,8] are capable of passively protecting mice against infections with different serotypes. PspA is, therefore, an attractive candidate for use as future protein-based pneumococcal vaccines.

Since *S. pneumoniae* enters the host primarily through the respiratory mucosa, vaccination strategies designed to target the airways are of great interest. An appropriate mucosal adjuvant is required to elicit an antigen-specific immune response in both the mucosal and systemic compartments [11]. We previously reported that each of the TLR agonists used in this study is an effective nasal adjuvant for the PspA antigen at a high dose (2.5 μg per mouse), and that it elicited the production of PspA-specific IgA in the airways and PspA-specific IgG in plasma. Because of this, it was capable of reducing the bacterial load in both the nasopharynx and lungs after a challenge with pneumococci with different serotypes [12]. Nasal immunization with a high dose of PspA alone could induce a certain level of PspA-specific IgG in the plasma and increased mouse survival, compared with mice that were nasally immunized with PBS alone, in a fatal pneumonia model in this study. These data suggest that nasal immunization with the reduced

***Corresponding author:** Kazunori Oishi, Laboratory for Clinical Research on Infectious Diseases, International Research Center for Infectious Diseases, Research Institute for Microbial Diseases, Osaka University, 3-1 Yamadaoka, Suita, Osaka 565-0871, Japan, Tel: 81-6-6879-4253; Fax: 81-6-6879-4255; E-mail: oishik@biken.osaka-u.ac.jp

Received January 28, 2011; **Accepted** March 14, 2011; **Published** March 19, 2011

Citation: Piao Z, Oma K, Ezoe H, Akeda Y, Tomono K, et al. (2011) Comparative Effects of Toll-Like Receptor Agonists on a Low Dose PspA Intranasal Vaccine against Fatal Pneumococcal Pneumonia in Mice. J Vaccines Vaccin 2:113. doi:10.4172/2157-7560.1000113

dose of PspA in combination with a TLR agonist was able to prevent the development of fatal pneumonia in this model. In the present study, we therefore examined the issue of whether nasal immunization using different TLR agonists in conjunction with a low dose (0.1μg per mouse) of PspA could confer protection against fatal pneumococcal pneumonia in healthy mice.

Materials and Methods

Mice and bacterial strains

Female C57BL/6 mice (6- to 8-wk-old) were purchased from Charles River Japan, Kanagawa, Japan. Mice were transferred to microisolators and maintained in horizontal laminar flow cabinets. They were provided sterile food and water in a specific pathogen-free facility. All mice used in these experiments were free of bacterial and viral pathogens. All animal experiments described in this study (protocol number; 08008) were performed in accordance with institutional guidelines for the Osaka University animal facility. *S. pneumoniae* WU2 strain with serotype 3, expressing PspA belonging to family 1, clade 2, was grown in Todd-Hewitt Broth (BD, Franklin Lakes, NJ) supplemented with 0.1% yeast extract (THY) to the mid-log phase and washed twice with phosphate-buffered saline (PBS) without $CaCl_2$ and $MgCl_2$. Bacteria were suspended in THY, and aliquots were snap frozen in liquid nitrogen and stored at -80°C until used.

Recombinant PspA and adjuvants

Recombinant PspA/Rx1 (amino acids 1 to 302) was prepared as previously described [8]. To extensively remove LPS from the PspA preparations, we used an LPS removal column, ProteoSpin^R, (Norgen, Thorold, Canada). Four TLR agonists, including *Escherichia coli* K12 LPS (TLR4 agonist), Pam3CSK4 (TLR1/2 agonist), Poly(I:C) (TLR3 agonist) or CpG ODN 1826 (TLR9 agonist) were selected to use as adjuvants. The LPS, Pam3CSK4 and Poly(I:C) were purchased from InvivoGen (san Diego, CA). CpG ODN 1826 was purchased from Hokkaido System Science (Sapporo, Japan). Each of these adjuvants was used in a dose of 10 μg for nasal immunization.

Nasal immunization

Mice were immunized intranasally three times at weekly intervals with 12μl of PBS containing 10μg of each TLR agonist and 0.1μg of PspA, 0.1μg of PspA alone or 12 μl of PBS on days 0, days 7 and days 14. The mice were euthanized on day 21 to obtain serum, bronchoalveolar lavage fluid (BALF) and a nasal wash (NW). The time points of nasal immunization and sampling for the determination of antibody levels were determined according to our previous study [13]. After removing the mandible, the nasal cavity was gently flushed with 1 ml of PBS from the posterior opening of the nose. The NW obtained from the anterior openings of the nose was collected. BALF was obtained by irrigation with 1 ml of PBS using a blunted needle inserted into the trachea after a tracheotomy [13].

PspA-specific antibody assays

PspA-specific antibody titers of IgG or IgA in Serum, BALF and NW were determined by ELISA as previously described [12]. PspA was used as the coating antigen (1 μg/ml). A 100μl sample was added to each well, followed by incubation at 37°C for 30 min. The plate was washed, and then reacted with 100μl of alkaline phosphatase-conjugated goat anti-mouse IgA, IgG, IgG1 or IgG2a (Zymed, San Francisco, CA) and the OD at 405 nm was then measured. End-point titers were expressed as the reciprocal $\log_2$ of the last dilution giving an OD_{405} of 0.1 OD unit above the OD_{405} of negative control samples obtained from non-immunized mice.

IgG binding and C3 deposition assays

Antibody binding was analyzed by whole cell ELISA. Frozen stock of *S. pneumoniae* WU2 (family 1 and clade 2) were plated onto blood agar, incubated overnight and then grown in THY to an OD_{600} of 0.4~0.5 and harvested by centrifugation. The bacterial cells were washed, resuspended in PBS, and fixed with 80% ethanol at room temperature for 1 h. The ethanol-killed bacteria were washed twice with PBS, and the pellet resuspended in PBS to an OD_{600} of about 0.2. 50μl of the ethanol-killed bacteria were coated in ELISA overnight at 4°C. The following day, the wells were washed 3 times with 0.05% of Tween-20 in PBS (PBST). The plates were then blocked with 3 % of skim milk in PBST at room temperature for 1 h. After 3 washes with PBST, 50μl of diluted serum in 1 % of skim milk in PBST were added to the plates, which were then incubated at 37°C for 2 h. The plates were washed 3 times with PBST, and then reacted with 100μl of alkaline phosphatase-conjugated goat anti-mouse IgG (Zymed, San Francisco, CA). The OD at 405 nm was then measured. The end-point titers were expressed as the reciprocal $\log_2$ of the last dilution giving an OD_{405} of 0.1 OD unit above the OD_{405} of negative control samples obtained from non-immunized mice.

C3 deposition was analyzed by flow cytometry. 10μl or 20μl of heat-inactivated serum was incubated with washed *S. pneumoniae* WU2 cells in 100μl of a reaction mixture achieving at a final concentration of 10^8 cfu/ml at 37°C for 30 min. The live bacteria were washed once with PBS and then incubated with 10% fresh normal mouse serum as the source of complement in gelatin veronal buffer with Ca^{2+} and Mg^{2+} (Sigma, St. Louis, MO) at 37°C for 30 min. After washing, live bacteria were incubated with 100μl of fluorescein isothiocyanate-conjugated anti-mouse C3 IgG (MP Biomedicals, Solon, OH) in PBS for 30 min on ice. The samples were fixed with 2% formaldehyde after two washing steps and stored at 4°C. Flow cytometry analysis was conducted using a FACSCalibur apparatus (Becton Dickinson), and 10,000 gated events were recorded.

Fatal pneumococcal pneumonia model

To determine the protective effects of nasal immunization with PspA plus each TLR agonist, *S. pneumoniae* WU2 strain at a dose of 2.0×10^7 cfu ($3 \times LD_{50}$) suspended in 30μl of sterile saline was intranasally administered to both the immunized and untreated mice 2 weeks after the last immunization. The 2-week interval between the last immunization and the bacterial challenge was maintained to avoid the influence of each TLR agonist on pulmonary defense, since some TLRs are involved in the innate immune response *to S. pneumoniae* [14-16]. The blood or lungs were aseptically removed from mice that had been anesthetized or euthanized with pentobarbital at 24 h post-bacterial challenge. The lung tissue was homogenized in 2 ml of sterile saline per whole lung tissue prior to culturing. To prevent coagulation, the blood was collected in tubes containing heparin. Quantitative bacterial cultures of blood or lung tissues were performed on horse blood agar. Mortality was monitored for 16 days following the pneumococcal challenge.

Statistics

Statistical analyses were performed using one-way ANOVA and Tukey's multiple comparison method for antibody titers and bacterial clearance [17], and a log rank (Mantel-Cox) test for analysis of the survival curve with Graphpad Prism (GraphPad Software, Sandiego,

CA). Data were considered to be statistically significant if the *p*-values were less than 0.05.

Results

Immune responses to PspA in mice after nasal immunization with a low dose of PspA plus TLR agonists

While no PspA-specific IgG was detected in sera of mice that had been immunized nasally with PspA alone, increased high levels of PspA-specific IgG were detected in sera of mice that had been immunized nasally with PspA plus and either LPS, Pam3CSK4, Poly(I:C) or CpG 1826 (Figure 1A). The levels of PspA-specific IgG in the sera of mice immunized PspA plus LPS were significantly higher than those of mice that had been immunized with PspA plus and either Poly(I:C) ($p < 0.01$) or CpG 1826 ($p < 0.01$). No significant difference was found among the levels of PspA-specific IgG among mice that had been immunized nasally PspA plus Pam3CSK4, Poly(I:C) or CpG 1826.

The levels of PspA-specific IgG in the BAL fluids and NWs of mice that had been nasally immunized with PspA plus the LPS were 5.17 ± 0.98 and 1.67 ± 1.03, respectively. In contrast, negligible levels of PspA-specific IgG were induced in the BAL fluids and NWs from mice that had been nasally immunized PspA plus Pam3CSK4, Poly(I:C) and CpG 1826. PspA-specific IgA was not detected in the BAL fluid or NWs from these mice that had been immunized nasally with PspA plus the TLR agonist.

No PspA-specific IgG1 or IgG2a was detected in sera of mice that had been immunized nasally with PspA alone (Figure 1B). In contrast, increased levels of PspA-specific IgG1 or IgG2a were found in mice that had been immunized nasally with PspA plus the TLR agonist. The levels of PspA-specific IgG1 in sera of mice that had been immunized nasally with PspA plus LPS were significantly higher than those of mice that were immunized nasally with PspA plus Pam3CSK4 ($p < 0.05$), PspA plus Poly(I:C) ($p < 0.01$) or PspA plus CpG 1826 ($p < 0.01$). No

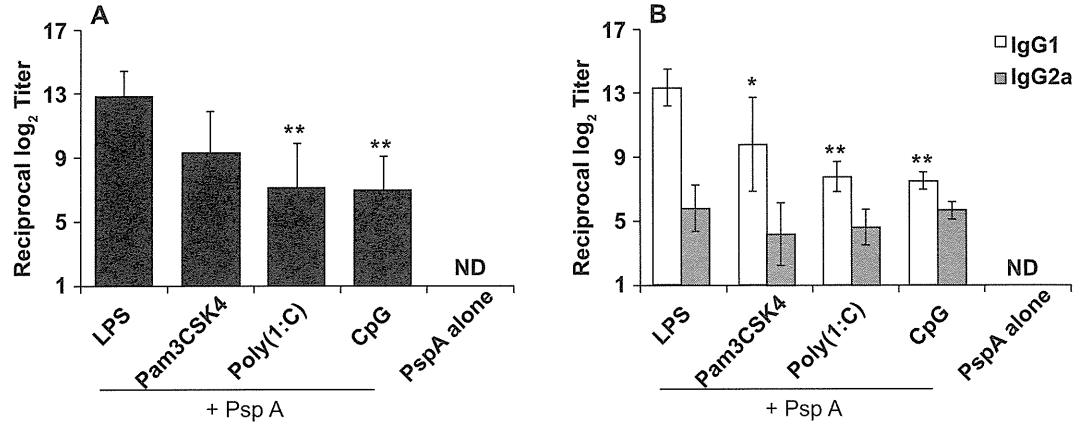

Figure 1: Induction of PspA-specific IgG (closed bars)(A), PspA-specific IgG1 (open bars) and IgG2a (gray bars) (B) in serum by intranasal immunization with either PspA plus each TLR agonist or PspA alone. Mice were nasally immunized three times at weekly intervals with 10 μg of TLR agonist and 0.1 μg of PspA. One week after the final immunization, the mice were euthanized to obtain serum, and PspA-specific antibody titers were determined using ELISA. The results are expressed as the mean ± S.D. for six mice per group. *$p < 0.05$, **$p < 0.01$, when compared with mice that were nasally immunized PspA plus LPS. ND, not detected.

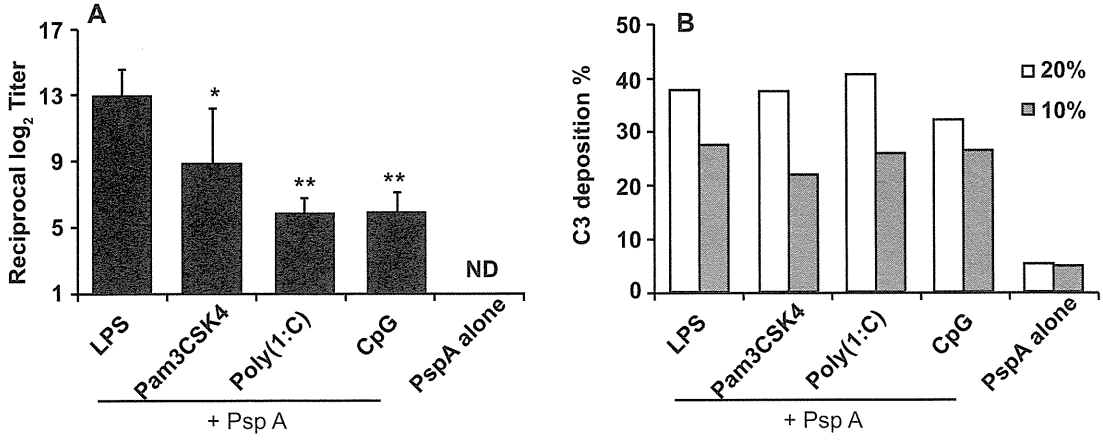

Figure 2: Binding of IgG antibodies (A) and C3 deposition (B) on the *S. pneumoniae* WU2 cell surface in the presence of sera from immunized and control mice. Binding The levels of IgG were analyzed by whole cell ELISA, and the C3 deposition were analyzed by flow cytometry using *S. pneumoniae* WU2 cells which were incubated with 20% (open bars) or 10% (gray bars) of pooled sera from mice that were immunized by intranasal immunization with either PspA plus each TLR agonist or PspA alone. The percentage of fluorescent bacteria (greater than 10 fluorescence intensity units) is shown as C3 deposition for each sample. *$p < 0.05$, **$p < 0.01$, when compared with mice that were nasally immunized PspA plus LPS. The results are expressed as the mean ± S.D. for six mice per group. ND, not detected.

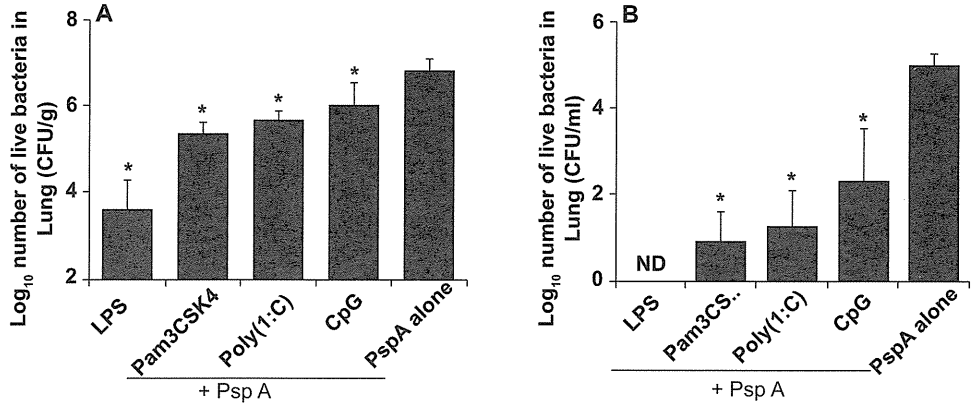

Figure 3: The effect of intranasal immunization with PspA plus each TLR against on the bacterial densities in Lung tissue (A) and blood (B) at 24 h post-challenge with the *S. pneumoniae* WU2 strain. An invasive dose of 2×10^7 cfu / mouse was nasally administered to mice that had been previously immunized with either PspA plus each TLR agaonist or PspA alone. Mice were euthanized to obtain lung tissues or blood from infected mice at the indicated time-point after bacterial challenge, and quantitative bacterial cultures of lung tissue or blood were performed. Values represent the Log_{10} cfu / g or Log_{10} cfu / ml (mean ± S.D.) for six mice per group. *$p < 0.0001$, when compared with mice that were nasally immunized with PspA alone.

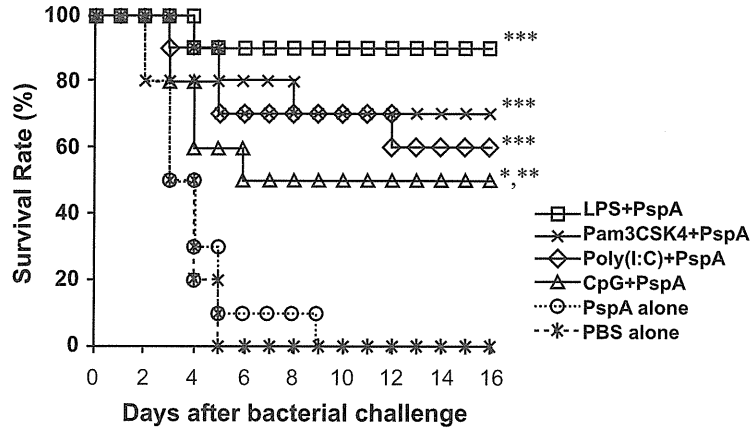

Figure 4: Survival of mice that were immunized nasally with a low dose of PspA plus each TLR agonist, a low dose of PspA alone and PBS alone after pneumococcal pneumonia. Immunized mice were intranasally challenged with 2×10^7 cfu of pneumococcal strain WU2, and the survival of the mice was monitored for 16 days. Results were examined by a Kaplan-Meier survival curve analysis for ten mice per group. *$p < 0.05$, when compared with mice that were nasally immunized PspA alone. **$p < 0.01$, when compared with mice that were nasally immunized PBS alone. ***$p < 0.001$, when compared with mice that were nasally immunized PspA alone or PBS alone.

significant difference was found in PspA-specific IgG1 levels among the sera of mice that were nasally immunized with PspA plus Pam3CSK4, Poly(I:C) or CpG 1826. No significant difference was found in PspA-specific IgG2a among sera of mice that were immunized nasally with PspA plus the TLR agonist. The mean ratios of PspA-specific IgG1 titers to PspA-specific IgG2a titers were 2.26 for LPS, 2.33 for Pam3CSK4, 1.68 for Poly(I:C), and 1.32 for CpG 1826, respectively.

IgG binding and C3 deposition on the bacterial surface

While no binding of mouse IgG was observed in the case of bacteria treated with sera from mice that were immunized nasally with PspA alone, the levels of mouse IgG found on bacteria that were treated with sera from mice immunized nasally with the PspA plus LPS, Pam3CSK4, Poly(I:C) or CpG 1826 (Figure 2A) was increased. The levels of mouse IgG were significantly higher in sera from mice that were immunized nasally PspA plus LPS compared to mice that were nasally immunized with PspA plus Pam3CSK4 ($p < 0.05$), PspA plus poly (I:C) or PspA plus CpG 1826 ($p < 0.01$). These levels of mouse IgG in serum from mice that were immunized nasally with PspA plus the TLR agonist closely corresponded with the levels of PspA-specific IgG induced in serum. The frequencies of C3 depositions were substantially increased in bacteria that had been pretreated with 10% and 20% sera from mice that were immunized nasally with PspA plus each of the TLR agonists, compared with those of mice that were immunized nasally with PspA alone (Figure 2B). No differences were found in the frequencies of C3 deposition on bacteria that were pretreated with sera from mice nasally immunized with PspA plus each TLR agonist.

Bacterial clearance from the lungs and the blood

The bacterial densities (mean ± S.D. for Log_{10} cfu / g) reached 6.83 ± 0.26 in the lung and 4.89 ± 0.3 in blood from mice that were immunized nasally with PspA alone at 24 h post-challenge (Figure 3A and 3B). Significant decreases were found in bacterial density in the lungs of mice that were immunized nasally with PspA plus either

LPS, Pam3CSK4, Poly(I:C) or CpG 1826 compared with mice that were immunized nasally with the PspA alone ($p < 0.0001$). No significant differences were found in the bacterial densities in the lung among mice immunized nasally with PspA plus LPS, Pam3CSK4, Poly(I:C) or CpG 1826 (Figure 3A). Significant decreases were also found in blood from mice that were immunized nasally with PspA plus either Pam3CSK4, Poly(I:C) or CpG 1826 compared with mice that were immunized nasally with the PspA alone ($p < 0.0001$). No bacteria were detected in blood samples from any of the mice that were immunized nasally with PspA plus LPS agonist. No significant differences were found among mice immunized nasally with PspA plus LPS, Pam3CSK4, Poly(I:C) or CpG 1826 (Figure 3B).

Protection by PspA plus each TLR vaccine against fatal pneumococcal pneumonia

As shown in Figure 4, the Kaplan-Meier analysis demonstrated significant protection as evidenced by the mean survival rate for mice that were immunized nasally with PspA plus each TLR agonist compared with mice that were immunized nasally with PspA alone or PBS alone. The survival rate was 90% for mice immunized nasally with the PspA plus LPS agonist ($p < 0.0001$ for PspA alone or PBS alone), 70% for mice immunized nasally with PspA plus Pam3CSK4 agonist ($p = 0.0008$ for PspA alone or $p = 0.0006$ for PBS alone), 60% for mice immunized nasally with PspA plus Poly(I:C) agonist ($p = 0.0005$ for PspA alone or $p = 0.0003$ for PBS alone), 50% for mice immunized nasally with PspA plus CpG 1826 agonist ($p = 0.0127$ for PspA alone or $p = 0.0062$ for PBS alone), respectively. No significant differences were found among mice that were immunized nasally with PspA plus LPS, Pam3CSK4, Poly(I:C) or CpG 1826.

Discussion

The findings reported herein provide a demonstration of the protective effects of the nasal vaccination of a low dose of PspA plus each TLR agonist against a fatal model of pneumococcal pneumonia with serotype 3 *S. pneumoniae* WU2. Nasal vaccination of a low dose of PspA plus each TLR agonist induced a high level of PspA-specific IgG in the serum and a low level of PspA-specific IgG in the airways of mice. The binding of PspA-specific IgG in sera resulted in an increase in C3 deposition on the bacterial surfaces. Subsequently, the bacterial densities in the lung tissues and blood were significantly decreased in mice that were immunized nasally with PspA plus TLR agonist, compared with the values for mice immunized nasally with a low dose of PspA alone. The reduction in bacterial densities in lung tissues could be explained by the sufficient extravasation of PspA-specific IgG into the alveolar space of mice that were immunized nasally with a low dose of PspA plus each TLR agonist [18]. Bacterial invasion into the blood circulation was readily suppressed by PspA-specific IgG in sera of mice immunized nasally with a low does of PspA plus each of the TLR agonists. The survival of infected mice that were immunized nasally with a low dose of PspA plus TLR agonist was significantly increased compared with those of mice that were immunized nasally with a low dose of PspA alone. These findings are in contrast with findings reported in our previous study, showing no significant difference in the survival of infected mice between nasal immunization with a high dose (2.5μg) of PspA plus TLR agonist and a high dose of PspA alone in a fatal pneumonia model using the WU2 strain [12]. The findings reported herein on the effect of a low dose of PspA plus TLR agonist also suggest possibilities for the development of a cost-effective PspA intranasal vaccine with the goal of preventing a fatal pneumonia.

We recently reported on the pivotal role of PspA-specific IgA on the bacterial clearance of a less virulent serotype 19F strain in the upper airway in a mouse model of bacterial colonization [19]. Since PspA-specific IgG was shown to be sufficient for protecting mice against a fatal bacteremic pneumonia caused by a virulent serotype 3 strain in this study, PspA-specific IgA may not be essential for invasive pneumococcal infections, such as bacteremic pneumonia.

While the rank orders of PspA-specific IgG induced in sera were LPS > Pam3CSK4 > Poly(I:C) and CpG 1826, no difference was found in the frequency of C3 deposition on bacterial surfaces in immune sera induced by a low dose of PspA plus each TLR agonist in this study. This discrepancy between the levels of PspA-specific IgG and the frequencies of C3 deposition may be explained by the similar ratios of PspA-specific IgG1 titers to IgG2a titers (1.32 to 2.33) among mice that were immunized nasally with a low dose of PspA plus each TLR agonist in this study, because the C3 binding activity of the IgG2a isotype is superior to those of other IgG isotypes [20]. Although antibacterial effects in the lung and blood were the highest in mice that were immunized nasally with a low dose of PspA plus LPS than those in mice immunized nasally with a low dose of PspA plus the other TLR agonists at 24 h post-infection, no significant difference was found in the survival rate of mice immunized nasally with a low dose of PspA plus each TLR agonist. This discrepancy may be explained by subsequent bacterial growth in the lungs and blood in mice that had been immunized nasally with a low dose of PspA plus LPS as well as mice immunized nasally with a low dose of PspA plus the other TLR agonists later than 24 h post-infection.

Despite similar C3 binding activities of immune sera, the rank orders for the survival rates of the immunized mice were LPS > Pam3CSK4 > Poly(I:C) and CpG 1826, and were in agreement with those of plasma levels of PspA-specific IgG reported in this study. Although LPS or Pam3CSK4 demonstrated a superior adjuvant effect among the TLR agonists tested in this study, these bacterial products are highly toxic to humans. In contrast, a synthetic analogue of a dsRNA compound, such as Poly (I:C) or Poly I:PolyC12 U (Ampligen^{R}), or CpG ODN would be expected to be applicable as a safe mucosal adjuvant in humans [21,22].

In conclusion, the data presented here provide evidence to indicate that intranasal immunization with a vaccine containing a low dose of PspA plus each TLR agonist elicited a high level of systemic PspA-specific IgG, and was capable of preventing the development of fatal pneumococcal pneumonia in mice. An intranasal administration of each TLR agonist in combination with a low dose PspA significantly increased the survival rates of the infected mice in the following order: LPS > Pam3CSK4 > Poly(I:C) and CpG ODN 1826. This study confers an important insight regarding strategies for a cost-effective PspA protein-based vaccine against invasive pneumococcal infections.

Acknowledgments

We are grateful to Dr. DE Briles and Dr. SK Hollingshead from the University of Alabama at Birmingham, for providing the pneumococcal strain and the recombinant plasmid, pUAB055, used in this study. This work was supported by the Program for Promotion of Fundamental Studies in Health Sciences of the National Institute of Biomedical Innovation (NIBIO), and by the Biomedical Cluster Kansai project, which is promoted by the Regional Innovation Cluster Program and subsidized by the Japanese Government, by the Global Center of Excellence Programs of Osaka University, and by Grants-in-Aid from the Ministry of Health, Labor and Welfare of Japan for "Mechanisms, epidemiology, prevention and control of acute respiratory infection".

References

1. Garau J (2002) Treatment of drug-resistant pneumococcal pneumonia. Lancet Infect Dis 2: 404-415.

2. Butler JC, Shapiro ED, Carlone GM (1999) Pneumococcal vaccines: history, current status, and future directions. Am J Med 107: 69S-76S.

3. Singleton RJ, Hennessy TW, Bulkow LR, Hammitt LL, Zulz T, et al. (2007) Invasive pneumococcal disease caused by nonvaccine serotypes among Alaska native children with high levels of 7-valent pneumococcal conjugate vaccine coverage. JAMA 297: 1784-1792.

4. Hicks LA, Harrison LH, Flannery B, Hadler JL, Schaffner W, et al. (2007) Incidence of pneumococcal disease due to non-pneumococcal conjugate vaccine (PCV7) serotypes in the united states during the era of widespread PCV7 vaccination, 1998-2004. J infect Dis 196: 1346-1354.

5. Briles DE, Tart RC, Swiatlo E, Dillard JP, Smith P, et al. (1998) Pneumococcal diversity: considerations for new vaccine strategies with emphasis on pneumococcal surface protein A (PspA). Clin Microbiol Rev 11: 645-657.

6. Tai SS (2006) *Streptococcus pneumoniae* protein vaccine candidates:properties, activities and animal studies. Crit Rev Microbiol 32: 139-153.

7. Briles DE, Hollingshead SK, King J, Swift A, Braun PA, et al. (2000) Immunization of humans with recombinant pneumococcal surface protein A (rPspA) elicits Abs that passively protect mice from fatal infection with *Streptococcus pneumoniae* Bearing Heterologous PspA. J Infect Dis 182: 1694-1701.

8. Nabors GS, Braun PA, Herrmann DJ, Heise ML, Pyle DJ, et al (2000) Immunization of healthy adults with a single recombinant pneumococcal surface protein A (PspA) variant stimulates broadly cross-reactive Abs to heterologous PspA molecules. Vaccine 18: 1743-1754.

9. Mcdaniel LS, Mcdaniel DO, Hollingshead SK, Briles DE (1998) Comparison of the PspA sequence from *Streptococcus pneumoniae* EF5668 to the previously identified PspA sequence from strain Rx1 and ability of PspA from EF5668 to elicit protection against pneumococci of different capsular types. Infect Immun 66: 4748-4754.

10. Mcdaniel LS, Ralph BA, Mcdaniel DO, Briles DE (1994) Localization of protection-eliciting epitopes on PspA of *Sterptococcus pneumoniae* between amino acid residues 192 and 260. Microb Pathogen 17: 323-337.

11. Freytag LC, Clements JD (2005) Mucosal adjuvants. Vaccine Rev 23: 1804-1813.

12. Oma K, Zhao J, Ezoe H, Akeda Y, Koyama H, et al. (2009) Intranasal immunization with a mixture of PspA and a Toll-like receptor agonist induces specific Abs and enhances bacterial clearance in the airways of mice. Vaccine 27: 3181-3188.

13. Kurita S, Koyama J, Onizuka S, Motomura K, Watanabe H, et al. (2006) Dynamics of dendritic cell migration and the subsequent induction of protective immunity in the lung after repeated airway challenges by nontypeable *Haemophilus influenzae* outer membrane protein. Vaccine 24: 5896-5903.

14. Malley R, Henneke P, Morse SC, Cieslewicz MJ, Lipstich M, et al. (2003) Recognition of pneumolysin by Toll-like receptors 4 confers resistance to pneumococcal infection. Proc Natl Acad Sci 100: 1966-1971.

15. Albiger B, Dahlberg S, Sandgren A, Wartha F, Beiter K, et al. (2007) Toll-like receptor 9 acts at an early stage in host defense against pneumococcal infection. Cell Microbiol 9: 633-644.

16. McNeela EA, Burke A, Neill DR, Baxter C, Fernandes VE, et al. (2010) Pneumolysin activates the NLRP3 inflammasome and promotes proinflammatory cytokines independently of TLR4. PLoS Pathogens 6: e1001191.

17. Stoline MR (1981) The status of multiple comparisons: simultaneous estimation of all pairwise comparisons in one-way ANOVA designs. Am Stat 35: 134-135.

18. Sato S, Ouellet N, Pelletiter I, Shimard M, Rancourt A, et al. (2002) Role of galectin-3 as an adhesion molecule for neutrophil extravasation during *Streptococcus pneumonia.* J Immunol 168: 1813-1822.

19. Fukuyama Y, King JD, Kataoka K, Kobayashi R, Gilbert RS, et al. (2010) Secretory-IgA antibodies play an important role in the immunity to *Streptococcus pneumoniae*. J Immunol 185: 1755-62.

20. Oishi K, Koles NL, Guelde G, Pollack M (1992) Antibacterial and protective properties of monoclonal antibodies reactive with *Escherichia coli* O111:B4 lipopolysaccharide: relation to antibody isotype and complement-fixing activity. J Infect Dis 165: 34-45.

21. Thompson KA, Strayer DR, Salvato PD, Thompson CE, Klimas N, et al. (1996) Results of a double-blind placebo-controlled study of the double-stranded RNA drug PolyI:PolyC_{12}U in the treatment of HIV infection. Eur J Clin Microbiol Infect Dis 15: 580-587.

22. Kodama S, Abe N, Hirano T, Suzuki M (2006) Safety and efficacy of nasal application of CpG oligodeoxynucleotide as a mucosal adjuvant. Laryngoscope 116: 331-335.

INFECTION AND IMMUNITY, July 2011, p. 2819–2828 Vol. 79, No. 7
0019-9567/11/$12.00 doi:10.1128/IAI.01360-10

The Nasal Dendritic Cell-Targeting Flt3 Ligand as a Safe Adjuvant Elicits Effective Protection against Fatal Pneumococcal Pneumonia▽

Kosuke Kataoka,[1,2,5] Kohtaro Fujihashi,[2]* Keita Oma,[4] Yoshiko Fukuyama,[2] Susan K. Hollingshead,[3] Shinichi Sekine,[5] Shigetada Kawabata,[6] Hiro-O Ito,[1] David E. Briles,[3] and Kazunori Oishi[4]

Department of Preventive Dentistry, Institute of Health Biosciences, The University of Tokushima Graduate School, Tokushima 770-8504, Japan[1]; Department of Pediatric Dentistry, Immunobiology Vaccine Center, Institute of Oral Health Research,[2] and Department of Microbiology,[3] The University of Alabama at Birmingham, Birmingham, Alabama 35294-0007; Laboratory for Clinical Research on Infectious Diseases, International Research Center for Infectious Diseases, Research Institute for Microbial Diseases, Osaka University, Suita, Osaka 565-0871, Japan[4]; and Departments of Preventive Dentistry[5] and Oral and Molecular Microbiology,[6] Graduate School of Dentistry, Osaka University, Osaka 565-0871, Japan

Received 23 December 2010/Returned for modification 27 January 2011/Accepted 23 April 2011

We have previously shown that a pneumococcal surface protein A (PspA)-based vaccine containing DNA plasmid encoding the Flt3 ligand (FL) gene (pFL) as a nasal adjuvant prevented nasal carriage of *Streptococcus pneumoniae*. In this study, we further investigated the safety and efficacy of this nasal vaccine for the induction of PspA-specific antibody (Ab) responses against lung infection with *S. pneumoniae*. C57BL/6 mice were nasally immunized with recombinant PspA/Rx1 (rPspA) plus pFL three times at weekly intervals. When dynamic translocation of pFL was initially examined, nasal pFL was taken up by nasal dendritic cells (DCs) and epithelial cells (nECs) but not in the central nervous systems, including olfactory nerve and epithelium. Of importance, nasal pFL induced FL protein synthesis with minimum levels of inflammatory cytokines in the nasal washes (NWs) and bronchoalveolar lavage fluid (BALF). NWs and BALF as well as plasma of mice given nasal rPspA plus pFL contained increased levels of rPspA-specific secretory IgA and IgG Ab responses that were correlated with elevated numbers of $CD8^+$ and $CD11b^+$ DCs and interleukin 2 (IL-2)- and IL-4-producing $CD4^+$ T cells in the nasal mucosa-associated lymphoid tissues (NALT) and cervical lymph nodes (CLNs). The *in vivo* protection by rPspA-specific Abs was evident in markedly reduced numbers of CFU in the lungs, airway secretions, and blood when mice were nasally challenged with *Streptococcus pneumoniae* WU2. Our findings show that nasal pFL is a safe and effective mucosal adjuvant for the enhancement of bacterial antigen (Ag) (rPspA)-specific protective immunity through DC-induced Th2-type and IL-2 cytokine responses.

Streptococcus pneumoniae is a leading human pathogen causing diseases ranging from otitis media to pneumonia, bacteremia, and meningitis. This bacterium, commonly termed the pneumococcus, can result in an estimated 1.6 million deaths per year worldwide, more than half of which are young children in developing countries (2). Although pneumococcal capsular polysaccharide and pneumococcal protein-capsular conjugate vaccines can provide protective immunity against pneumonia and invasive diseases in adults and infants, a strong need still exists for a new generation of effective vaccines for the prevention of all potential *S. pneumoniae* infections. In this regard, the multivalent polysaccharide vaccines do not provide protection against strains with nonvaccine serotypes (28, 41). Of importance, pneumococcal surface protein A (PspA) has been extensively investigated as a candidate vaccine antigen (Ag) to prevent pneumococcal infection (5, 37). For instance, PspA-specific antibody (Ab) enhances bacterial clearance and induces cross-protection against infection with strains of different serotypes (4, 31). Further, previous studies have demonstrated that PspA-specific Abs overcome the anticomplementary effect of PspA, allowing increased complement activation and C3 deposition on PspA-bearing bacteria (27, 30).

Nasal immunization has been shown to preferentially induce Ag-specific Ab responses in the respiratory tract (20) and other mucosal lymphoid tissues (10, 25, 26). To induce maximal levels of Ag-specific immune responses in both mucosal and systemic lymphoid tissue compartments, it is often necessary to use a mucosal adjuvant (16, 22, 39). Although native cholera toxin and related *Escherichia coli* enterotoxin are potent mucosal adjuvant for enhancement of Ag-specific immune responses, their application for human use is not warranted since they can cause diarrhea or Bell's palsy (6, 23, 29). Moreover, these toxins are known to migrate into and accumulate in the olfactory tissues when given nasally (40). In this regard, our previous studies demonstrated that nasal application of a DNA plasmid (pFL) containing the gene of the Flt3 ligand (FL), which is a kind of cytokine, preferentially expanded $CD8^+$ dendritic cells (DCs) and subsequently induced Ag-specific mucosal immune responses mediated by interleukin 4 (IL-4)-producing $CD4^+$ T cells when mice were nasally administrated ovalbumin with pFL as the mucosal adjuvant (19). Further, a combination of nasal pFL and CpG oligonucleotides as a

* Corresponding author. Mailing address: Departments of Pediatric Dentistry and Microbiology, IVC, Institute of Oral Health Research, The University of Alabama at Birmingham, 1919 7th Avenue South, School of Dentistry Building 801A1, Birmingham, AL 35294-0007. Phone: (205) 934-1951. Fax: (205) 975-4431. E-mail: kohtarof@uab.edu.

▽ Published ahead of print on 2 May 2011.

double DNA adjuvant enhanced mucosal and systemic immune responses via induction of plasmacytoid DCs as well as $CD8^+$ DCs in mucosal compartments (11, 17). Nasal administration of an adenovirus vector encoding FL cDNA also showed enhancement and maintenance of long-term immunity (17, 32).

In this study, we examined the safety and effectiveness of nasal pFL as a mucosal adjuvant for the induction of functional bacterial Ag (recombinant PspA [rPspA])-specific Ab responses for protection against *S. pneumoniae* infection in the lower respiratory tract. Our findings show that nasal rPspA plus pFL adjuvant successfully elicits protective immunity in both the upper and lower respiratory tracts by enhancing mucosal DC-mediated Th2-type and IL-2 cytokine responses without detectable cytokine-mediated inflammation.

MATERIALS AND METHODS

Mice. Specific-pathogen-free female C57BL/6 mice (6 to 8 weeks old) were purchased from Charles River Japan (Kanagawa, Japan) and used in this study. Upon arrival, these mice were transferred to microisolators, maintained in horizontal laminar flow cabinets, and provided sterile food and water as part of a specific-pathogen-free facility at Osaka University (Suita, Japan), and all experiments were conducted in accordance with the guidelines provided by Osaka University. All of the mice used in these assays were free of bacterial and viral pathogens.

rPspA and adjuvants. Endotoxin-free rPspA was purified by chromatography on a chelating Sepharose 4B column preloaded with Ni^+ (GE Healthcare, Piscataway, NJ) from *Escherichia coli* BL21(DE3) carrying pUAB055, which comprised the first 302 of the 588 amino acids of PspA/Rx1, including all of the α-helical region and some of the proline-rich region (3). The plasmid pORF9-mFlt3L (pFL) consists of the pORF9-mcs vector (pORF) plus the full-length murine FL cDNA gene (InvivoGen, San Diego, CA). These plasmids were purified using the Gene Elute endotoxin-free plasmid kit (Sigma-Aldrich, St. Louis, MO) (19). The Limulus amebocyte lysate assay (BioWhittaker, Walkersville, MD) resulted in <0.1 endotoxin unit of lipopolysaccharide (LPS) per 1 μg of plasmids or rPspA.

Nasal immunization and sample collection. Mice were immunized three times at weekly intervals nasally with 6 μl/nostril phosphate-buffered saline (PBS) containing 5 μg of rPspA and 50 μg of pFL as a mucosal adjuvant. As controls, mice were immunized nasally with 50 μg of pORF (empty plasmid) and 5 μg of rPspA under anesthesia. In some experiments, mice were administered pFL (50 μg), pORF (50 μg), rPspA (1 μg or 5 μg), native cholera toxin (nCT) (1 μg), or PBS alone under anesthesia. Plasma, nasal washes (NWs), and bronchoalveolar lavage fluid (BALF) were obtained as described previously (36).

Dynamic translocation of pFL. On 12 h or 7 days after mice were nasally given pFL (50 μg) alone, mononuclear cells were isolated from nasal mucosa-associated lymphoreticular tissues (NALT) and nasal passages (NPs) as described previously (14, 19), and NALT and NP dendritic cells (DCs) were purified by the AutoMACS cell sorter (Miltenyi Biotec, Auburn, CA) using anti-CD11c monoclonal Ab (MAb) microbeads (19). Further, nasal epithelial cells (nECs) and olfactory nerves and epithelium (ON/E) were isolated from nasal passages and olfactory bulbs, respectively (14, 40). In brief, cells from the nasal mucosa and olfactory bulb were prepared by gentle teasing through stainless screens and were subjected to discontinuous gradient centrifugation using 40% and 55% Percoll. Cells on the surface of the 40% layer were used as nECs and ON/E. To further confirm the presence of nECs and ON/E, the size and granularity of cells were determined by using flow cytometry. DNA was then extracted from NALT, NP-DCs, nECs, and ON/E, and the ampicillin resistance gene (858 bp) contained in the pFL plasmid was detected by a primer-specific PCR method. The sense primer was 5′-CCA ATG CTT AAT CAG TGA GGC-3′, and the anti-sense primer was 5′-ATG AGT ATT CAA CAT TTC CGT GTC G-3′. The PCR products were separated by electrophoresis in 2% agarose gels and visualized by UV light illumination following ethidium bromide (0.5 mg/ml) staining (19).

Analysis of FL protein synthesis. Twelve hours after nasal administration of pFL (50 μg), empty plasmid (50 μg), rPspA alone, or PBS, DCs from NALT and NPs and nECs and ON/E were purified aseptically as described above and were then cultured for 48 h (2×10^6 cells/ml) in complete medium. The concentrations of FL protein secreted into the medium were determined by FL-specific enzyme-linked immunosorbent assay (ELISA) (Quantikine M mouse Flt3 ligand ELISA kit; R & D Systems, Minneapolis, MN). Mice were next nasally immunized weekly for three consecutive weeks with rPspA (5 μg) plus pFL (50 μg) or pORF (50 μg), rPspA alone (5 μg), or PBS, and 1 week after the last immunization, the FL protein in nasal washes (NWs) and bronchoalveolar lavage fluid (BALF) was determined by FL-specific ELISA (R & D Systems).

Detection of inflammatory cytokines in mucosal secretion. In order to determine inflammatory cytokines by nasal application of pFL, NWs and BALF were collected 5 days after the nasal administration of pFL (50 μg), pORF (50 μg), rPspA (1 μg or 5 μg), or native cholera toxin (1 μg). Next, the mucosal secretion samples were subjected to ELISA specific to IL-1β, IL-6 (R & D Systems), and tumor necrosis factor alpha (TNF-α) according to the manufacturer's instructions (eBioscience, San Diego, CA).

rPspA-specific Ab assays. In order to examine mucosal and systemic immune responses to Ag, rPspA-specific IgA and IgG antibody (Ab) levels in plasma, NWs, and BALF were determined by ELISA on day 7 after the last immunization, as described previously (18, 19, 32). Briefly, 96-well Falcon microtest assay plates (BD Biosciences, Oxnard, CA) were coated with 1 μg/ml of rPspA in PBS. After incubating serial dilutions of samples, horseradish peroxidase-conjugated goat anti-mouse IgM, IgG, IgG1, IgG2a, IgG2b, IgG3, or IgA (Southern Biotechnology Associates Inc., Birmingham, AL) was added to wells. The color reaction was developed for 15 min at room temperature. Endpoint titers were expressed as the reciprocal $\log_2$ of the last dilution that gave an optical density at 415 nm (OD_{415}) of 0.1 greater than the background level. Further, mononuclear cells obtained from spleen, NALT, cervical lymph nodes (CLNs), mediastinal lymph nodes (MeLNs), NPs, and lungs were subjected to an enzyme-linked immunospot (ELISPOT) assay in order to determine the numbers of Ag-specific Ab-forming cells (AFCs) (18, 19). In brief, mononuclear cells in the spleen, NALT, CLNs, and MeLNs were isolated aseptically by a mechanical dissociation method using gentle teasing through stainless steel screens as described previously (14). For isolation of mononuclear cells from NPs, a modified dissociation method was used based upon a previously described protocol (18). Mononuclear cells from lungs were isolated by a combination of an enzymatic dissociation procedure with collagenase type IV (0.5 mg/ml; Sigma-Aldrich) followed by discontinuous Percoll (Amersham Biosciences, Arlington Heights, IL) gradient centrifugation.

Flow cytometric analysis. To characterize the phenotype of DCs, aliquots of mononuclear cells (0.2×10^6 to 1.0×10^6 cells) were isolated from various lymphoid compartments 1 week after the last immunization with rPspA plus pFL or pORF. The cells were stained with fluorescein isothiocyanate (FITC)-conjugated anti-mouse CD11b, CD8, or B220 MAbs (BD Biosciences). In some experiments, mononuclear cells were incubated with phycoerythrin (PE)-labeled anti-mouse $I\text{-}A^b$, CD11c, CD40, CD80, or CD86 MAbs (BD Biosciences) and biotinylated anti-mouse CD11c MAbs (BD Biosciences), followed by CyChrome-streptavidin. These samples were then subjected to flow cytometry analysis (FACSCalibur; BD Biosciences) for cell subset analysis (19).

rPspA-specific $CD4^+$ T cell responses and cytokine-specific ELISA. $CD4^+$ T cells from lungs, CLNs, and spleen were purified using an automatic cell sorter (AutoMACS) system (Miltenyi Biotec) as described previously (18, 19). The purified $CD4^+$ T cell fraction (>97% $CD4^+$ and >99% viable) was resuspended in RPMI 1640 (Sigma-Aldrich) supplemented with HEPES buffer (10 mM), L-glutamine (2 mM), nonessential amino acid solution (10 μl/ml), sodium pyruvate (10 mM), penicillin (100 U/ml), streptomycin (100 μg/ml), gentamicin (80 μg/ml), and 10% fetal calf serum (FCS) (complete medium; 4×10^6 cells/ml) and cultured in the presence of T cell-depleted, complement- and mitomycin-treated splenic Ag-presenting cells taken from nonimmunized, normal mice with or without 2 μg/ml rPspA. To assess rPspA-specific T cell proliferative responses, an aliquot of 0.5 μCi of tritiated [^{3}H]TdR (PerkinElmer Japan Co., Ltd., Japan) was added during the final 18 h of incubation, and the amount of [^{3}H]TdR incorporation was determined by scintillation counting (19). The culture supernatants were collected on day five and analyzed using gamma interferon (IFN-γ)-, IL-2-, IL-4-, IL-5-, IL-6-, and IL-10-specific ELISA kits (eBioscience). The detection limit for each cytokine was as follows: 15 pg/ml for IFN-γ, 2 pg/ml for IL-2, 4 pg/ml for IL-4, IL-5, and IL-6, and 30 pg/ml for IL-10.

Pneumococcal infection. Mice were nasally challenged with a serotype 3 *S. pneumoniae* strain (WU2) with a mucoid phenotype at a dose of 1.8×10^7

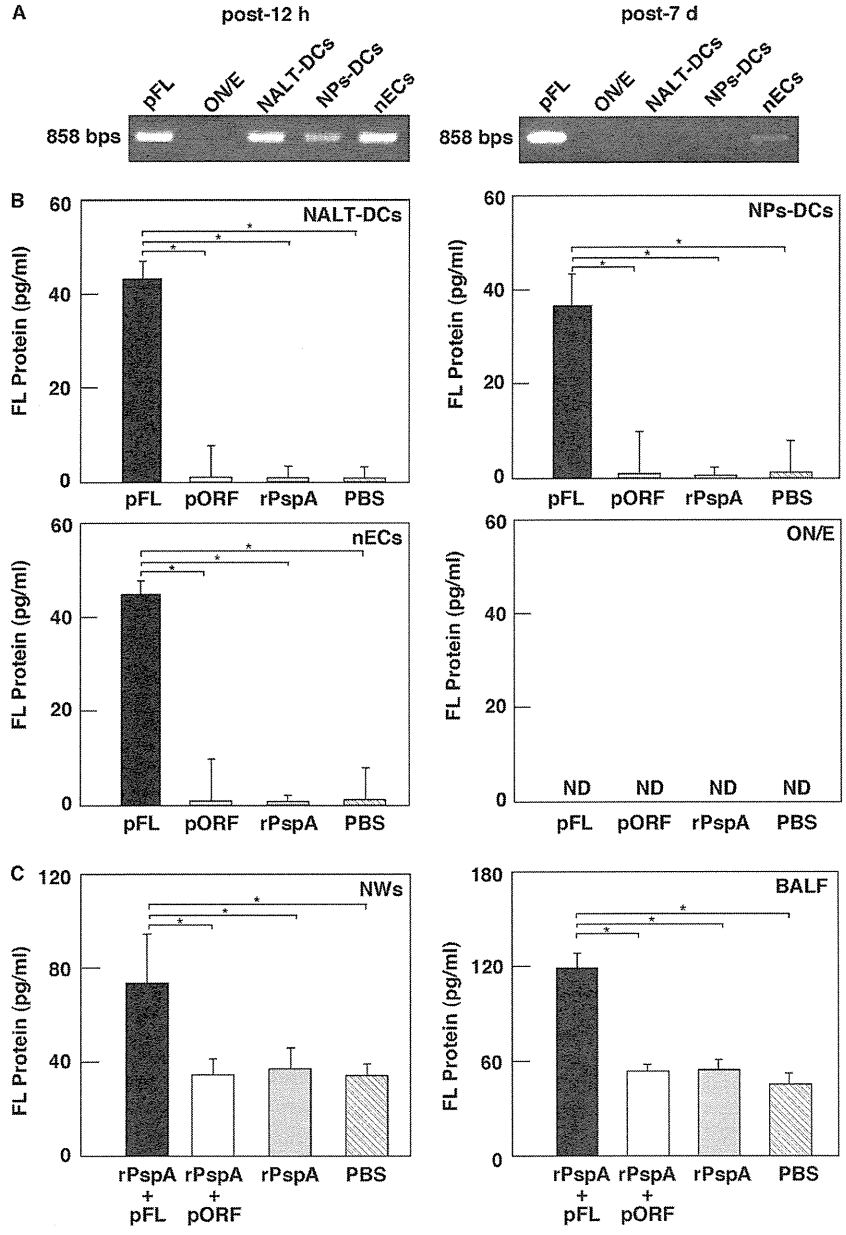

FIG. 1. (A to C) Translocation of FL plasmid after nasal administration of pFL (A), FL protein production by nasal DCs and epithelial cells (B), and expression of the FL protein in mucosal secretions (C). (A) Twelve hours (left) or 7 days (right) after nasal application of pFL (50 μg), the DNA samples were extracted from 1.0×10^5 (each) cells of the olfactory nerve and epithelium (ON/E; lane 2), NALT-DCs (lane 3), NPs-DCs (lane 4), and nasal epithelial cells (nECs; lane 5). In order to show the presence of plasmid in these cell populations, the ampicillin resistance gene (858 bp) contained in pFL was detected by PCR using specific primers. pFL (0.1 μg) was employed as a positive control (lane 1). (B) Mice were nasally administered pFL (50 μg; black column), pORF (50 μg; white column), rPspA (5 μg; shaded column), or PBS (hatched column). Twelve hours later, NALT-DCs, NPs-DCs, nECs, and ON/E were isolated and cultured (2×10^6 cells/ml, respectively) for 48 h in complete medium. The concentration of FL protein secreted in medium was measured by FL-specific ELISA. The values shown are the means ± SEM for 30 mice for each group and a total of three experiments. *, $P < 0.05$ compared with results for the mouse group given pORF, rPspA, or PBS. (C) Mice were nasally immunized weekly for three consecutive weeks with rPspA (5 μg) plus pFL (50 μg; black column) or pORF (50 μg; white column), rPspA alone (5 μg; shaded column), or PBS (hatched column). One week after the last immunization, NWs and BALF (100 μl, respectively) were collected and subjected to FL-specific ELISA. The values shown are the means ± SEM of data for 30 mice for each group and a total of three experiments. *, $P < 0.05$ compared with results for mouse group given pORF, rPspA, or PBS.

CFU (20 μl). Forty-eight hours after the bacterial challenge, the lungs were removed aseptically and homogenized in 9 ml of sterile saline per gram of lung tissues. NWs and blood were collected as described above. Bacterial colonies were counted by plating lungs, NWs, and blood (50 μl, respectively) on horse blood agar (BD Biosciences), followed by incubation at 37°C overnight. The detection limit of bacterial culture was 10^2 CFU/g. The 50% lethal dose was calculated to be 2.5×10^6 CFU.

Statistical analysis. Each result is expressed as the mean ± 1 standard error of the mean (SEM). All mouse groups were compared with control mice using an unpaired Mann-Whitney U test by using the Statview software program

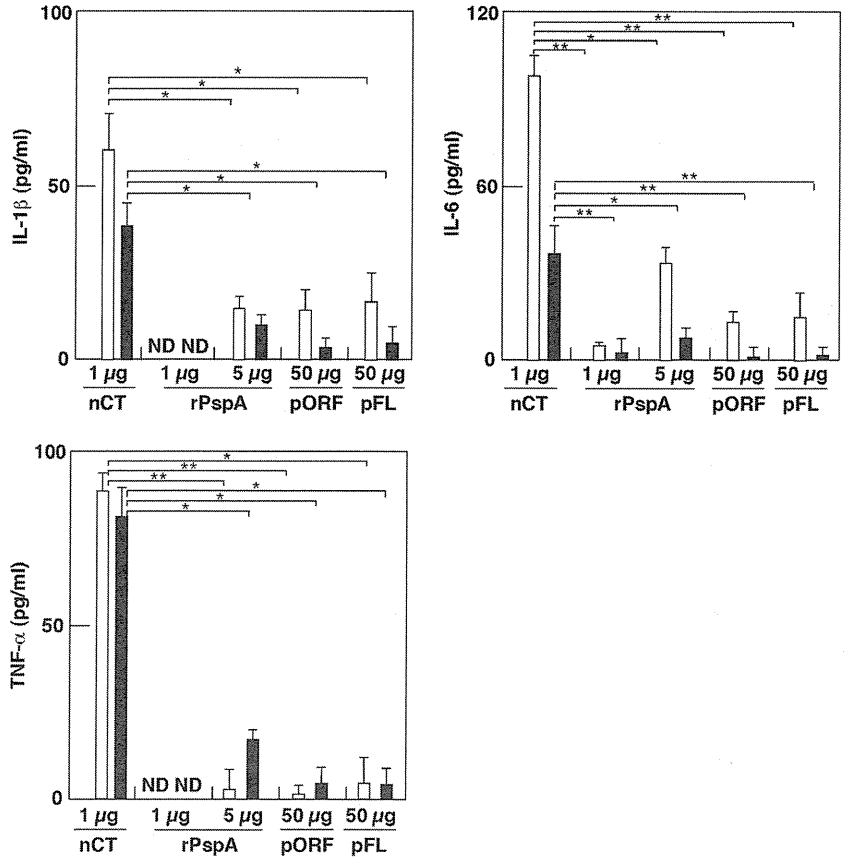

FIG. 2. Inflammatory cytokine production in NWs (white column) and BALF (black column). Mice were nasally administered native cholera toxin (nCT) (1 μg), rPspA (1 or 5 μg), pORF (50 μg), or pFL (50 μg). Five days later, NWs and BALF were collected and subjected to IL-1β-, IL-6-, and TNF-α-specific ELISA. The values shown are the means ± SEM of data for 30 mice for each group and total of three experiments. *, $P < 0.05$; **, $P < 0.01$ (compared with results for mouse group given nCT).

(Abacus Concepts, Cary, NC), designed for Macintosh computers, with Bonferroni's correction. P values of <0.05 or <0.01 were considered significant.

RESULTS

Tracking plasmid expression and FL protein synthesis. In order to examine safety of pFL for nasal application, we initially traced plasmid-specific ampicillin resistance gene expression by nasal DCs, nECs, and the ON/E. DCs from NALT and NPs, as well as nECs, possessed the ampicillin resistance gene 12 h after nasal administration of pFL (Fig. 1A, left). Of interest, on 7 days after nasal pFL application, the ampicillin resistance gene was detected only in nECs (Fig. 1A, right). Further, NALT-DCs, NP-DCs, and nECs of mice given nasal pFL produced significantly elevated levels of the FL protein compared with those of mice given nasal pORF (empty plasmid), rPspA alone, or PBS (Fig. 1B). In addition, nasal application of the combination of rPspA and pFL resulted in FL protein production comparable to that with nasal application of pFL alone (data not shown). However, FL protein synthesis in mice given nasal rPspA plus pORF was at essentially the same level as that seen in mice given pORF or rPspA alone (data not shown). Thus, NWs and BALF from mice given nasal pFL plus rPspA contained significantly higher levels of FL than those from mice given nasal pORF plus rPspA, rPspA alone, or PBS only (Fig. 1C). On the other hand, of importance, no plasmid-specific genes were essentially detected in the ON/E of mice given nasal pFL (Fig. 1A). Thus, the culture supernatants of ON/E did not contain detectable levels of the FL protein (Fig. 1B). These results show that pFL is largely present in nasal DCs and nECs but not in the ON/E and suggest that pFL on nECs may maintain production of the FL protein.

Nasal pFL induces lower levels of inflammatory cytokines than nCT. Although pFL was not taken up by the central nervous system, it is important to show that FL produced in the nasal cavity does not induce inflammatory responses. In this regard, the levels of IL-1β, IL-6, and TNF-α production in NWs and BALF were examined 5 days after nasal administration with rPspA, pORF, native cholera toxin (nCT), or pFL. The levels of inflammatory cytokine synthesis in NWs and BALF of mice given nasal pFL were essentially the same as or lower than that of mice given nasal rPspA or pORF alone (Fig. 2). Similarly, nasal application of rPspA plus pFL resulted in low levels of inflammatory cytokine production which were similar to those seen in pFL alone (data not shown). Conversely, nasal nCT induced markedly high levels of these inflammatory cytokines (Fig. 2). These results show that nasal pFL application does not elicit unnecessary inflammatory responses in the nasal mucosa.

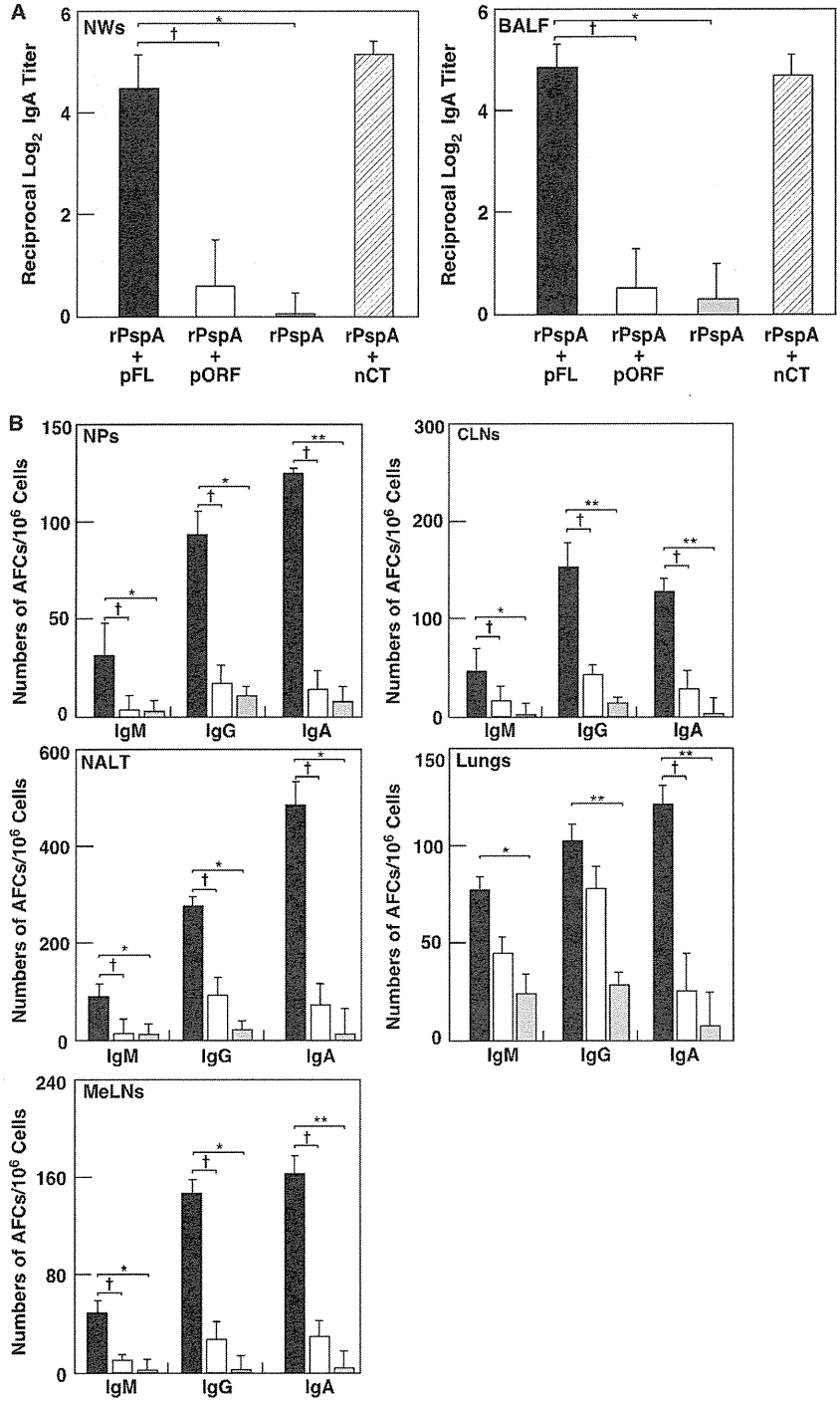

FIG. 3. Mucosal immune responses to rPspA in external secretions and mucosal lymphoid tissues. C57BL/6 mice were nasally immunized three times at weekly intervals with rPspA (5 μg) plus pFL (50 μg; black column) or pORF (50 μg; white column), rPspA alone (shaded column), or rPspA (5 μg) plus nCT (1 μg; hatched column). (A) Seven days after the last immunization, the levels of rPspA-specific IgA Abs in NWs and BALF were determined by rPspA-specific ELISA. (B) Seven days after the last immunization, mononuclear cells isolated from NPs, CLNs, NALT, lungs, and MeLNs were subjected to ELISPOT assay to determine the numbers of Ag-specific IgM, IgG, and IgA Ab-forming cells (AFCs). The values shown are the means ± SEM ($n = 20$). *, $P < 0.05$; **, $P < 0.01$ (compared with mouse group given rPspA alone). †, $P < 0.05$ (compared with mouse group given rPspA plus pORF).

Induction of rPspA-specific Ab responses in mucosal and systemic tissues of mice given rPspA plus pFL. We next examined whether nasal administration of pFL as a mucosal adjuvant would enhance rPspA-specific Ab responses. Giving mice nasal rPspA plus pFL resulted in significantly increased levels of rPspA-specific IgA Ab responses in NWs and BALF compared with results for mice given nasal rPspA plus pORF or rPspA Ag alone (Fig. 3A). The levels of rPspA-specific IgA

Ab responses for mice given rPspA plus pFL were comparable to those seen for mice given nasal nCT vaccination (Fig. 3A). To further support these findings, elevated numbers of PspA-specific IgA AFCs were detected in NPs, CLNs, NALT, lungs, and MeLNs of mice given nasal rPspA and pFL (Fig. 3B). In addition, significantly higher numbers of rPspA-specific IgG and/or IgM AFCs were seen for mice given pFL as a nasal adjuvant than for mice given nasal pORF or rPspA alone (Fig. 3B). These results clearly show that pFL as a nasal adjuvant effectively elicits rPsp-specific Ab responses in mucosa-associated lymphoid tissues in the respiratory tract. Since nasal immunization is known to induce systemic immunity in addition to the mucosa, rPspA-specific Ab responses in plasma and spleen were examined. Nasal pFL as a mucosal adjuvant successfully enhanced rPspA-specific IgG and IgA Ab responses in plasma which are comparable to those responses seen in mice given nasal rPspA plus nCT (Fig. 4A). Thus, significantly increased numbers of rPspA-specific IgM, IgG, and IgA AFCs were seen in spleen of mice given pFL as a nasal adjuvant (Fig. 4B). When the levels of rPspA-specific IgG subclass Ab responses were examined, increased levels of anti-rPspA IgG1, IgG2a, and IgG2b Abs were noted for mice given nasal rPspA plus pFL compared with those Ab responses for mice given rPspA plus pORF or rPspA alone (Fig. 4A). Essentially no IgG3 Ab response against rPspA was detected. Taken together, pFL as a nasal adjuvant effectively induces rPspA-specific Ab responses in both mucosal and systemic immune compartments.

Nasal rPspA plus pFL leads CD11b$^+$ and CD8$^+$ DCs. Since our previous studies reported that nasal pFL plus ovalbumin as an Ag elicited expansion of CD8-expressing lymphoid-type CD11c$^+$ DCs (19), we next characterized CD11c$^+$ DCs in the various mucosal tissues of mice given rPspA plus pFL or pORF. Nasal immunization of rPspA plus pFL significantly increased the frequency of CD11c$^+$ cells in both mucosal and systemic tissues compared with results for mice given rPspA plus pORF (Table 1). Interestingly, the numbers of CD8$^+$ DCs were increased in all tissues of mice given pFL as a nasal adjuvant compared with those numbers for mice given nasal pORF. In addition, increased frequencies of CD11b$^+$ DCs were noted in NALT, NPs, CLNs, and spleen. In contrast, increased frequencies of B220$^+$ DCs were seen only in CLNs (Table 1). Further, higher expression of major histocompatibility complex class II (MHC II), CD40, CD80, and CD86 was seen on CD11c$^+$ DCs (Table 1). CD8$^+$ and CD11b$^+$ DCs from NALT, lungs, and NPs were also examined by fluorescence-activated cell sorting (FACS) for expression of costimulatory molecules. Our results showed increased frequencies of costimulatory molecule expression by CD8$^+$ and CD11b$^+$ DCs in the tissues of mice given nasal pFL compared with those in control groups (Table 2). Taken together, these results indicate that nasal administration of rPspA plus pFL preferentially expands the numbers of CD8$^+$ and CD11b$^+$ DC populations which express elevated levels of costimulatory molecules.

Th1- and Th2-type cytokine responses by PspA-specific CD4$^+$ T cells. We next assessed rPspA-specific CD4$^+$ T cell responses induced by pFL as a mucosal adjuvant. rPspA-stimulated CD4$^+$ T cells from lungs, CLNs, and spleen of mice given nasal rPspA plus pFL showed significantly higher proliferative responses than did those from mice nasally immunized

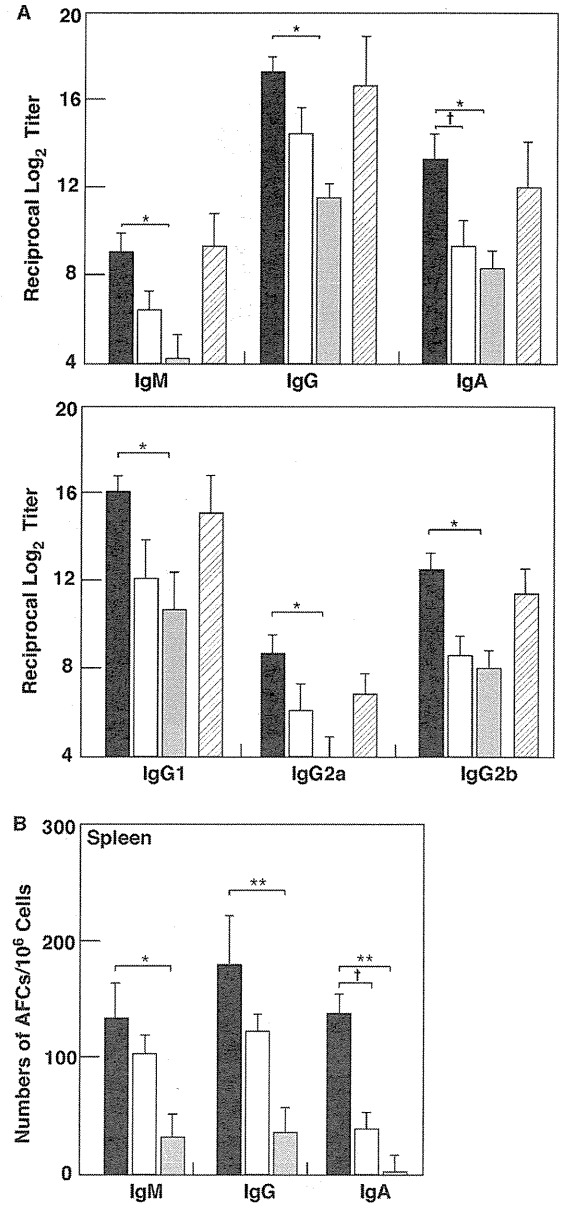

FIG. 4. Comparison of rPspA-specific Ab responses in plasma and spleen cells of mice given nasal rPspA plus pFL (black column) or pORF (white column), rPspA alone (shaded column), or rPspA plus nCT (hatched column). Each mouse group was nasally immunized weekly for three consecutive weeks. (A) Seven days after the last immunization, rPspA-specific IgM, IgG, IgA, and IgG subclass Ab responses in plasma were determined by Ag-specific ELISA. An rPspA-specific IgG3 Ab response was not detected. (B) Seven days after the last immunization, mononuclear cells were isolated from spleens and were then subjected to ELISPOT assay to determine numbers of rPspA-specific IgM, IgG, and IgA AFCs. The values shown are the means ± SEM (n = 20). *, $P < 0.05$; **, $P < 0.01$ (compared with results for mouse group given rPspA alone). †, $P < 0.05$ (compared with results for mouse group given rPspA plus pORF).

with rPspA plus pORF (Table 3). In this regard, when Th1- and Th2-type cytokine profiles were examined, PspA-stimulated CD4$^+$ T cells from mice given pFL as a nasal adjuvant exhibited higher levels of IL-2, IL-4, IL-5, and IL-6 production than those in control mice. On the other hand, levels of IFN-γ